Sucrose-induced Receptor Kinase SIRK1 Regulates a Plasma Membrane Aquaporin in Arabidopsis*[S]

Xu Na Wu‡, Clara Sanchez Rodriguez‡, Heidi Pertl-Obermeyer‡, Gerhard Obermeyer§, and Waltraud X. Schulze‡¶

The transmembrane receptor kinase family is the largest protein kinase family in Arabidopsis, and it contains the highest fraction of proteins with yet uncharacterized functions. Here, we present functions of SIRK1, a receptor kinase that was previously identified with rapid transient phosphorylation after sucrose resupply to sucrose-starved seedlings. SIRK1 was found to be an active kinase with increasing activity in the presence of an external sucrose supply. In *sirk1* T-DNA insertional mutants, the sucrose-induced phosphorylation patterns of several membrane proteins were strongly reduced; in particular, pore-gating phosphorylation sites in aquaporins were affected. SIRK1-GFP fusions were found to directly interact with aquaporins in affinity pull-down experiments on microsomal membrane vesicles. Furthermore, protoplast swelling assays of *sirk1* mutants and SIRK1-GFP expressing lines confirmed a direct functional interaction of receptor kinase SIRK1 and aquaporins as substrates for phosphorylation. A lack of SIRK1 expression resulted in the failure of mutant protoplasts to control water channel activity upon changes in external sucrose concentrations. We propose that SIRK1 is involved in the regulation of sucrose-specific osmotic responses through direct interaction with and activation of an aquaporin via phosphorylation and that the duration of this response is controlled by phosphorylation-dependent receptor internalization. ***Molecular & Cellular Proteomics 12: 10.1074/mcp.M113.029579, 2856–2873, 2013.***

The growth and development of a plant require precise control of carbon and nitrogen assimilation, as well as controlled allocation between growth and storage functions. In plants, sucrose and starch are the main products of photosynthesis. Besides its function as the main carbon transport metabolite connecting producing source tissues with consuming sink tissues such as growing regions and storage organs (1), sucrose also serves as an important metabolite with signaling functions in many aspects of plant physiology (2–5). Sucrose as a signal requires the perception of external and internal sucrose status, as well as some signal transduction pathways induced by alterations in sucrose availability.

Sucrose synthesis and degradation are highly regulated (4, 6–8). The mechanisms of sucrose uptake across the plasma membrane have been studied extensively in the past (9–13), and with the characterization of the sugar-exporting SWEET transporter family (14), our understanding of the path for sucrose across the plasma membrane is fairly complete. However, despite the importance of sucrose as a metabolite and metabolic signal (15), many aspects of sucrose-related signaling and the mechanisms involved in controlling sucrose transport remain poorly understood. Regulatory effects of sucrose have been studied in a systematic manner through the analysis of sucrose-induced transcriptional changes (16), the sucrose-starvation-induced translational status of mRNAs (17), or ribosome subunit composition (18). However, only a few genes have been characterized that are regulated by sucrose specifically (19). Examples of sucrose-specific transcriptional responses are those of the bZIP transcription factor family (5, 20). A sensing mechanism for membrane-localized sucrose involving sucrose transporters has been suggested (21, 22). Even if the sucrose-sensing mechanisms were cytosolic, as has been suggested for glucose (23), the responses likely also would involve the modulation of transport processes at the plasma membrane.

Furthermore, sucrose and other nutrients are also osmotically active, and exposure to altered osmotic conditions requires cellular adjustments. A histidine receptor kinase has been identified as an osmosensor in plants (24), but the involvement of other kinases and of hormone signaling pathways in osmotic responses also has been demonstrated (25–27). Thus, plant cells, although protected by a rigid cell wall system, are required to mount an integrated response to the combination of nutritional and osmotic alterations in their external environment. In this respect, a universal means of osmotic regulation is the regulation of water fluxes across the plasma membrane. Aquaporins, the water channels

From the ‡Max Planck Institute for Molecular Plant Physiology, Am Mühlenberg 1, 14476 Golm, Germany; §Molecular Plant Biophysics and Biochemistry, Department of Molecular Biology, University of Salzburg, Billrothstraβe 11, 5020 Salzburg, Austria; ¶Department of Plant Systems Biology, University of Hohenheim, 70593 Stuttgart, Germany

Received April 21, 2013, and in revised form, June 30, 2013
Published, MCP Papers in Press, July 2, 2013, DOI 10.1074/mcp.M113.029579

present in all cellular organisms, provide a means of fast regulation upon osmotic stress (28–30) and are tightly regulated by phosphorylation (31).

Reversible phosphorylation is a key mechanism for regulating protein function in all organisms (32, 33). Regarding the regulation of sucrose metabolism, posttranslational regulation through the phosphorylation of sucrose phosphate synthase has been elucidated (34). Furthermore, there are indications of the regulation of sucrose transport through phosphorylation (35, 36), although the precise functions of the phosphorylation events remain to be determined. In the past decade, a number of systematic medium- to large-scale mass-spectrometry-based phosphoproteomics studies have resulted in the identification of protein phosphorylation sites, and the magnitude of phosphorylation in many cases was condition dependent (37–42). Particularly, sucrose-induced protein phosphorylation was analyzed in a time course experiment in which sucrose was resupplied to sucrose-starved Arabidopsis seedlings (43), and comprehensive information about the phosphorylation sites of Arabidopsis proteins can be found in the PhosPhAt database (44, 45). However, we still know little about the kinases in plants that are responsible for phosphorylation of the large number of experimentally identified phosphorylation sites. Targets for recombinant expressed plant kinases have been experimentally screened for via either exposure to a substrate peptide mixture and subsequent mass spectrometric analysis of peptide phosphorylation (46) or protein or peptide arrays (47, 48). In Arabidopsis, a number of kinase–substrate relationships have been identified through genetic interactions based on crosses of different mutants (see various examples in Ref. 49).

Up to now, only a few of the large-scale phosphoproteomic studies had been followed by more detailed studies on the role of particular phosphoproteins in the context of the stimulus. Here, we carried out a systematic functional study on one of the receptor kinases (SIRK1) identified from a large-scale analysis of sucrose-induced protein phosphorylation (43). We used gene expression mutants and phosphorylation site-directed mutants in combination with proteomic, physiological, and cell biological experiments to characterize the *in vivo* role of this protein kinase in the context of sucrose resupply after starvation responses.

EXPERIMENTAL PROCEDURES

Plant Material—A T-DNA insertional mutant for *sirk1* (SALK_125543) was identified within the SALK T-DNA insertional lines collection (50). Seeds of *sirk1* T-DNA insertional mutant were obtained from the Nottingham Arabidopsis Stock Centre and propagated in the greenhouse at the Max Planck Institute for Molecular Plant Physiology (Potsdam, Germany). The *sirk1* T-DNA insertional mutant carries a T-DNA insertion in the first intron of *SIRK1* and was confirmed via PCR amplification using T-DNA border primer LBb1.3 (5′-ATTTTGCCGATTTCGGAAC-3′) and gene-specific primer SIRK1-RP (5′-GTGGGTTTCCTAGTGGCTTTC-3′). The expression of *SIRK1* in the wild type and *sirk1* mutant was examined by using a pair of gene-specific primers (SIRK1–1F, 5′-TTTCGAGGTTCACGTGCAAG-3′ and SIRK1–1R, 5′-CCTATATCCCCAGGCAGCATAC-3′).

Quantitative Real-time PCR—Total RNA was extracted from the *sirk1* plants using the Plant RNA Mini Kit (Invitek, Berlin, Germany) according to the instructions provided by the manufacturer. RNA was digested with DNaseI (Roche Diagnostics, Germany) to remove the genomic DNA. First-strand cDNA was synthesized using SuperScript III reverse transcriptase (Invitrogen). Quantitative real-time PCR analysis was performed using the StepOnePlus Real Time PCR system (Applied Biosystems, Austin, TX) with the SYBR green detection protocol (Applied Biosystems, Austin, TX). The UBQ gene was used as an internal control, and the relative expression of the gene of interest was calculated using a comparative Δ-Δ C_t method (51). Primers for *SIRK1* were designed for the N-terminal part (F1/R1) and the C-terminal part of the gene (F2/R2): F1 5′-TTTCGAGGTTCACGTGCAAG-3′, R1 5′-CCTATATCCCCAGGCAGCATAC-3′; F2 5′-TTGCCAATAATAAGCTGTCCGC-3′, R2 5′-CGACACATTGAATCCCACCATT-3′. Primers used for ubiquitin were 5′-GGCCTTGTATAATCCCTGATGAATAAG-3′ and 5′-AAAGAGATAACAGGAACGGAAACATAGT-3′.

SIRK1 Overexpression and Mutagenesis Constructs—Full-length cDNA of the *SIRK1* gene without a stop code was amplified via PCR using the specific forward primer SIRK1-EcoRI (5′-G*GAATTC*ATGAGTCATTTTCTCACTTTCTG-3′) and the specific reverse primer AtSIRK1-SmaI (5′-ACAA*CCCGGG*AGCAGGCAGAAATTGAAGTA-3′). It was then subcloned into the pGEM-T easy vector (Promega, Fitchburg, WI). The EcoRI-*SIRK1*-SmaI fragment was then cloned into the plant transformation vector pEZR(H)-LN (a kind gift from Staffan Persson Lab, Max Planck Institute for Molecular Plant Physiology) upstream and as a fusion of the GFP coding sequence, resulting in the plasmid ^{35}S::AtSIRK1-GFP. The construct pGEM-T easy-EcoRI-*SIRK1*-SmaI was used for mutating Ser-744 of AtSIRK1 to Ala-744 or Asp-744. Site-directed mutagenesis was done via PCR using specific primer pairs (5′-GTTAGATGTTTACgCACCTGATAGATTGGC-3′ and 5′-CCAATCTATCAGGTGcGTAAACATCTAAC-3′ or 5′-GTTAGATGTTTACgatCCTGATAGATTGGC-3′ and 5′-CAATCTATCAGGatcGTAAACATCTAACAT-3′) and the QuikChange II Site-Directed Mutagenesis Kit (Agilent Technologies, Santa Clara, CA). The EcoRI-*AtSIRK1^{S744A}*-SmaI fragment or EcoRI-*SIRK1^{S744D}*-SmaI fragment also was cloned into plant transformation vector pEZR(H)-LN and as a fusion with the GFP coding sequence, resulting in the plasmid ^{35}S::AtSIRK1^{S744A}-GFP or ^{35}S::AtSIRK1^{S744D}-GFP. Three plasmids were transferred into *Agrobacterium tumefaciens* strain GV3101, and *sirk1* mutant plants were transformed using the floral dip method (52). Homozygous T_2 transgenic lines were further selected by means of segregation analysis, and T_3 seeds were used for experiments. The fluorescence of GFP in the transgenic lines was checked via confocal laser-scanning microscopy (TCS SP5, Leica Microsystems CMS GmbH, Wetzlar, Germany).

Seedling Growth and Experimental Design—*Arabidopsis* seedlings of wild type (col-0), *sirk1*, ^{35}S::AtSIRK1-GFP/*sirk1*, ^{35}S::AtSIRK1^{S744A}-GFP/*sirk1*, and ^{35}S::AtSIRK1^{S744D}-GFP/*sirk1* were germinated and grown under continuous light (20 °C, 130 μE/s*m^2) in Jouanneau and Péaud-Lenoël medium composed of micro- and macronutrients (53), with a total of 3 mM nitrogen and supplemented with 0.5% sucrose. After 11 days, we sucrose starved the seedlings by changing the growth medium to a sucrose-free medium and leaving the flasks in the dark for 24 h as described elsewhere (43). Sucrose was then resupplied to a final concentration of 30 mM for 3 min before seedlings were harvested for microsomal protein preparation. In a control experiment, 30 mM mannitol was used instead of sucrose.

Microsomal Preparation—A total of 4 g of seedlings (fresh weight) was homogenized in a falcon tube with 20 ml extraction buffer (330 mM mannitol, 100 mM KCl, 1 mM EDTA, 50 mM Tris-MES, fresh 5 mM DTT, and 1 mM PMSF, pH 8) in the presence of 0.5% v/v proteinase inhibitor mixture (Sigma-Aldrich, Germany) and phosphatase inhibitors (25 mM NaF, 1 mM Na_3VO_4, 1 mM benzamidin, 3 μM leupeptin).

The homogenate was centrifuged for 15 min at 10,000 × *g* at 4 °C. The pellet was discarded, and the supernatant was ultracentrifuged for 1 h at 48,000 × *g* at 4 °C. The microsomal pellet was re-suspended in 100 μl of membrane buffer (330 mM mannitol, 25 mM Tris-MES, 0.5 mM DTT). The soluble fraction in the supernatant was precipitated with three times volume acetone overnight, and then proteins were resuspended in 500 μl 6 M urea, 2 M thiourea, pH 8.

Pull-downs of GFP-tagged SIRK1 and SIRK1S744 Mutants—Microsomal proteins (300 μg) isolated as described above were incubated with 50 μl of anti-GFP magnetic beads (Chromotek, Martinsried, Germany) for two hours on a rotating wheel at 4 °C. After incubation, the beads were collected on a μMACS separator (Milteniy Biotech, Bergisch-Gladbach, Germany) and washed two times with 350 μl and 500 μl wash buffer (10 mM Tris/HCl pH 7.5, 150 mM NaCl, 0.5 mM EDTA, 0.01% Nonidet P-40).

For protein–protein interaction assays, the proteins were eluted from the beads with 100 μl 6 M urea, 2 M thiourea, pH 8, before in-solution tryptic digestion. For kinase activity assays, one more washing step was carried out with wash buffer (10 mM Tris/HCl, pH 7.5, 300 mM NaCl, 0.5 mM EDTA), and the beads were mixed with 100 μl kinase reaction buffer (20 mM HEPES pH 7, 10 mM $MgCl_2$, 2 mM DTT, 0.1 mg ml^{-1} BSA).

Kinase Activity Assay—SIRK1-GFP fusion protein was affinity purified over magnetic beads (see above). A luciferase-based kinase activity assay was performed in 60 μl reaction mixture incubated for one hour at room temperature. The reaction mixture contained 20 μl to 40 μl beads with GFP-tagged proteins, 15 μl myelin basic protein (1 mg ml^{-1}; Sigma-Aldrich) as a generic kinase substrate, 1 μl of 40 μM ATP, and an appropriate reaction buffer (20 mM HEPES pH 7, 10 mM $MgCl_2$, 2 mM DTT, 0.1 mg ml^{-1} BSA). After incubation, 60 μl Kinase-Glo® Plus Reagents (Promega, Fitchburg, WI) were added and incubated for 10 min. Luminescence as a measure of ATP consumption was recorded with a luminometer (Microbeta Trilux). In general, protein isolations from three independent batches of seedlings were tested, and the average activity value plus/minus the standard deviation is presented.

In Vitro Peptide Phosphorylation—SIRK1-GFP fusion protein was affinity purified over magnetic beads (see above). A luciferase-based kinase activity assay was performed as described above, except that 30 μg of a mixture of putative target peptides was used as a substrate. The peptide mixture consisted of 25 peptides bearing experimentally confirmed phosphorylation sites to different proteins (including ALGSFGSFGSFR/PIP2F (AT2G39010), LGTVSSPEPISVVR/SWEET11 (AT3G48740), and LIEEVSHSSGSPNPVSD/AT3G02880), as well as control peptides without known phosphorylation sites (*e.g.* DPPPAPFFDMEELR/PIP2F (AT2G39010), TSPHLGEK/SWEET11 (AT3G48740), and INLGENK/AT3G02880). In total, the 43 peptides (supplemental Table S5) were exposed as a substrate to the enriched SIRK1-GFP fusions enriched in microsomal fractions of three independent protein isolations. After exposure to the target peptides, the reaction mixture was purified over C8 material to trap undigested SIRK1 protein and to collect the respective target peptides. Collected peptide mixtures were then desalted over C18 prior to mass spectrometric analysis. The phosphorylation of target peptides was confirmed via mass spectrometry (see below).

Protoplast Generation—Arabidopsis seedlings were grown in liquid cultures and sucrose starved as described above but not challenged with sucrose. Instead, parts of the 12-day-old seedlings were carefully dried on tissue paper, washed with a filter-sterilized 300 mM mannitol–10 mM $CaCl_2$ solution, and cut into small pieces that were finally transferred to 3 ml enzymatic digestion medium (ES-500M: 500 mM mannitol, 10 mM MES/KOH (pH 5.8), 10 mM $CaCl_2$, 10 mM KCl) plus 1% (w/v) cellulase Onozuka R10 (Duchefa, Haarlem, The Netherlands) and 1% (w/v) macerozyme R10 (Duchefa, The Netherlands). The protoplasts were prepared in the dark with gentle shaking for two to three hours, filtered through a 50-μm nylon filter, centrifuged at 80 × *g* at 4 °C for 5 min, and washed three times with ice-cold ES-500 M without enzymes. Protoplasts were stored in the dark on ice for at least 30 min before an experiment was started.

Protoplast Swelling Assays—In principle, protoplast swelling experiments were performed as described previously (54), with some modifications. Approximately 20 μl of the protoplast suspension were pipetted into 200 μl ES-500 M in a perfusion chamber mounted on the stage of an inverted microscope. Protoplasts were allowed to settle down for about 5 to 10 min. The chamber was then perfused with 3 ml of ES-500 M to select protoplasts sticking well to the glass bottom of the chamber. The perfusion solution was then changed to a hypo-osmolar solution (ES-350M) containing the same ingredients as ES-500 M but with 350 mM mannitol instead of 500 mM mannitol. The solution change in the chamber lasted about 15 s. Images were taken every 3 s with a video-camera-equipped microscope for a total of 300 s. In some experiments, protoplasts were treated with 30 mM sucrose. For this, the chamber was perfused with a solution containing 30 mM sucrose and 470 mM mannitol (ES-470M_30S) for about 5 min (ES-470M_30S: 470 m M mannitol, 30 mM sucrose, 10 mM MES/KOH (pH 5.8), 10 mM $CaCl_2$, 10 mM KCl) and then challenged with a hypo-osmolar solution consisting of 320 mM mannitol and 30 mM sucrose (ES-320M_30S: 320 mM mannitol, 30 mM sucrose, 10 mM MES/KOH (pH 5.8), 10 mM $CaCl_2$, 10 mM KCl). The osmolality of all media was measured with a cryoscopic osmometer (Osmomat 030, Gonotec, Berlin, Germany), and the following osmolalities were noted: ES-500M, 0.578 Osmol kg^{-1}; ES-470M_30S, 0.588 Osmol kg^{-1}; ES-350M, 0.402 Osmol kg^{-1}; ES-320M_30S, 0.395 Osmol kg^{-1}.

The diameter of the protoplasts was measured using imageJ software. Diameters were converted to micrometers, and the volume, surface area, and relative volume were calculated for each time point. A regression line was fitted to the steepest part of the swelling curve to determine the maximal water volume flux density, which corresponds to aquaporin activity. Statistical analysis was performed with Sigma Plot (Jandel Scientific, San Rafael, CA).

Confocal Microscopy and Imaging Processing—Seedlings expressing SIRK1-GFP, $SIRK1^{S744A}$-GFP, and $SIRK1^{S744D}$-GFP were imaged on a confocal microscope equipped with a CSU-X1 Yokogawa spinning disc head fitted to a Nikon Ti-E inverted microscope, a CFI APO 60× water immersion objective, an evolve charge-coupled device camera (Photometrics Technology, Tucson, AZ), and a 1.2× lens between the spinning disc and the camera. GFP was excited at 491 nm and FM4-64 at 561 nm using a multichannel dichroic and an ET525/50 M or ET595/50 M band pass emission filter (Chroma Technology, Bellow Falls, VT) for GFP and red fluorescent protein, respectively. Image acquisitions were performed using Metamorph Online Premier, version 7.5. Typical exposure times were 600 ms for GFP and 300 ms for red fluorescent protein.

Four-day-old seedlings grown in the dark in half-strength MS liquid medium were incubated in half-strength MS liquid medium supplemented with 20 μM FM4-64 (stock solution: 4 mM in DMSO; Invitrogen, Molecular Probes) for 10 min. They were washed three times for 5 min in half-strength MS liquid medium. The treatments were performed in the dark under slight agitation.

The quantification of endocytotic events was performed for seedlings (four days old, grown in the dark in half-strength MS liquid medium) not incubated in FM4-64 in order to avoid any alteration of the sugar perception produced by the lipophilic dye. The three SIRK1 constructs (SIRK1-GFP, $SIRK1^{S744A}$-GFP, and $SIRK1^{S744D}$-GFP) were imaged directly after growth under sucrose-starvation conditions or after 3 to 15 min of sucrose resupply. Per treatment and genotype, at least eight seedlings and 20 hypocotyl cells/seedling were counted, starting from the bottom part of the hypocotyl. The

cells were classified according to the amount of endocytotic events observed—no detectable, few (less than 10 per cell), or many (more than 10 per cell)—as described elsewhere (55). All images were processed using ImageJ software. Background correction was performed using the Subtract Background tool (rolling ball radius: 50 pixels).

Protein Preparation for Mass Spectrometry—Microsomal or soluble proteins were predigested for 3 h with endoproteinase Lys-C (0.5 μg/μl; Wako Chemicals, Neuss, Germany) at room temperature. After 4-fold dilution with 10 mM Tris-HCl (pH 8), samples were digested with 4 μl sequencing-grade modified trypsin (0.5 μg μl^{-1}; Promega, Fichtburg, WI) overnight at 37 °C. After overnight digestion, trifluoroacetic acid (TFA)[1] was added (until the pH was 3 or less) to stop digestion. Digested peptides were desalted over a C18 tip (56) and dissolved in 100 μl 80% acetonitrile and 0.1% TFA before phosphopeptide enrichment with titanium dioxide (TiO_2) (GL Sciences, Torrance, CA).

Phosphopeptide Enrichment—Phosphopeptides were enriched over TiO_2 as described elsewhere (57), with some modifications. TiO_2 beads were equilibrated with 100 μl of 5% acetonitrile and 0.1% TFA. 100 μl digested and desalted peptides were mixed with 100 μl 5% acetonitrile and 0.1% TFA and incubated for about 1 min with 2 mg equilibrated TiO_2 beads. The solution with the beads was then placed into a self-made microcolumn in a 200-μl pipette tip with a C8 disc as a plug. Phosphopeptides were eluted from TiO_2 beads in these microcolumns using 5% ammonium hydroxide and 5% piperidine (58). Elutes were immediately acidified by adding 50 μl 20% phosphoric acid to reach a pH value less than 3. Enriched phosphopeptides were desalted over a C18 stage tip again prior to mass spectrometric analysis.

LC-MS/MS of Peptides and Phosphopeptides—Tryptic peptide mixtures were analyzed via LC-MS/MS using nanoflow Easy-nLC (Thermo Scientific) as an HPLC system and an Orbitrap hybrid mass spectrometer (LTQ-Orbitrap, Thermo Scientific) as a mass analyzer. Peptides were eluted from a 75-μm analytical column (Reprosil C18, Dr. Maisch GmbH, Tübingen, Germany) on a linear gradient running from 4% to 64% acetonitrile over 90 min and sprayed directly into the LTQ-Orbitrap mass spectrometer. Proteins were identified via MS/MS based on the information-dependent acquisition of fragmentation spectra of multiple charged peptides. Up to five data-dependent MS/MS spectra were acquired in the linear ion trap for each full-scan spectrum acquired at 60,000 full-width half-maximum resolution in the Orbitrap. The overall cycle time was approximately 1 s. When analyzing samples after phosphopeptide enrichments, multistage activation was chosen for fragmentation to achieve the simultaneous fragmentation of parent ion and neutral loss peaks of phosphopeptides (59).

Protein identification and ion intensity quantitation were carried out by MaxQuant, version 1.3.0.5 (60). Spectra were matched against the Arabidopsis proteome (TAIR10, 35,386 entries) using Andromeda (61). Common contaminants (trypsin, keratin, etc.) were included during database searches. Carbamidomethylation of cysteine was set as a fixed modification, and the oxidation of methionine and phosphorylation of serine, threonine, and tyrosine were set as variable modifications. Trypsin was specified as the protease, and up to two missed cleavages were allowed. The mass tolerance for the database search was set to 20 ppm for full scans and 0.5 Da for fragment ions. The multiplicity was set to 1. For label-free quantitation, retention time matching between runs was chosen within a time window of 2 min. Peptide and protein false discovery rates were set to 0.01, and the site false discovery rate was set to 0.05. The location of phosphorylation sites was determined by the site-scanning algorithm within Andromeda. Hits to contaminants (*e.g.* keratins) and reverse hits identified by MaxQuant were excluded from further analysis. A full list of all identified peptides from the phosphoproteomics experiment is found in supplemental Table S1, and that for the pull-down experiments is presented in supplemental Table S2. The identified phosphopeptides, including their spectra (supplemental Fig. S1), were submitted to the phosphorylation site database PhosPhAt (44, 45) and are publicly available.

Mass Spectrometric Data Analysis and Statistics—Reported ion intensity values were used for quantitative data analysis. cRacker (62) was used for label-free data analysis of phosphopeptide ion intensities based on the MaxQuant output. All phosphopeptides and proteotypic non-phosphopeptides were used for quantitation. Within each sample, ion intensities of each peptide ions species (each *m/z*) were normalized against the total ion intensities in that sample (peptide ion intensity/total sum of ion intensities). Subsequently, each peptide ion species (*i.e.* each *m/z* value) was scaled against the average normalized intensity of that ion across all treatments. For each peptide, values from three biological replicates were averaged after normalization and scaling. In the case of non-phosphopeptides, protein ion intensity sums were calculated from normalized scaled ion intensities of all proteotypic peptides.

Sucrose-induced phosphorylation was expressed as the ratio of normalized and scaled phosphopeptide ion intensity values at 3 min of sucrose resupply to the normalized and scaled phosphopeptide ion intensity values from the sucrose-starved control. For estimation of the sample-to-sample variation of sucrose-induced phosphorylation within each plant line, distributions of sucrose-induced phosphorylation ratios (normalized ion intensity at 3 min/normalized ion intensity at 0 min) were compared within col-0, within *sirk1*, and between *sirk1*/col-0 (supplemental Fig. S2), as described previously (63). Differences between the ratio distributions were assessed via a Kolmogorov-Smirnov test using the software R.

For the analysis of pull-down results, protein ion intensity values from three biological replicates in samples of bait pull-down and GFP-only pull-down were compared by means of a pairwise *t* test, and multiple testing correction (64) was applied. For pull-downs under sucrose-induced conditions, GFP-only pull-downs under sucrose-induced conditions were used as a control, and for the sucrose-starvation condition, GFP-only pull-downs under sucrose-starvation conditions were used as reference (supplemental Table S4).

Functional classification of proteins was done based on MAPMAN (65). Information about subcellular location was derived from the consensus location available from SUBA3 (66). For data not derived from mass spectrometry studies, statistical analyses were carried out using Sigma Plot (Jandel Scientific, San Rafael, CA) and Excel (Microsoft, Redmond, WA).

RESULTS

SIRK1 (AT5G10020), a member of the LRR-receptor-like kinase family, showed a significant transient increase in protein phosphorylation of serine 744 after sucrose resupply to sucrose-starved cells (43). In order to study the role of SIRK1 in sucrose-induced phosphorylation processes, we made use of a *sirk1* T-DNA insertional mutant (SALK_125543). The T-DNA was inserted into the first intron of the *SIRK1* gene (Fig. 1*A*). Homozygous mutants of *sirk1* were selected from a segregating population using a PCR screen with gene-specific primers and T-DNA primers (Fig. 1*B*). Homozygous *sirk1* mutants had an overall reduced *SIRK1* gene expression (Fig. 1*C*). Additionally, no peptides of SIRK1 protein were fragmented in membrane preparations of *sirk1* T-DNA insertional mutants,

[1] The abbreviations used are: EVC, empty vector control; TFA, trifluoroacetic acid.

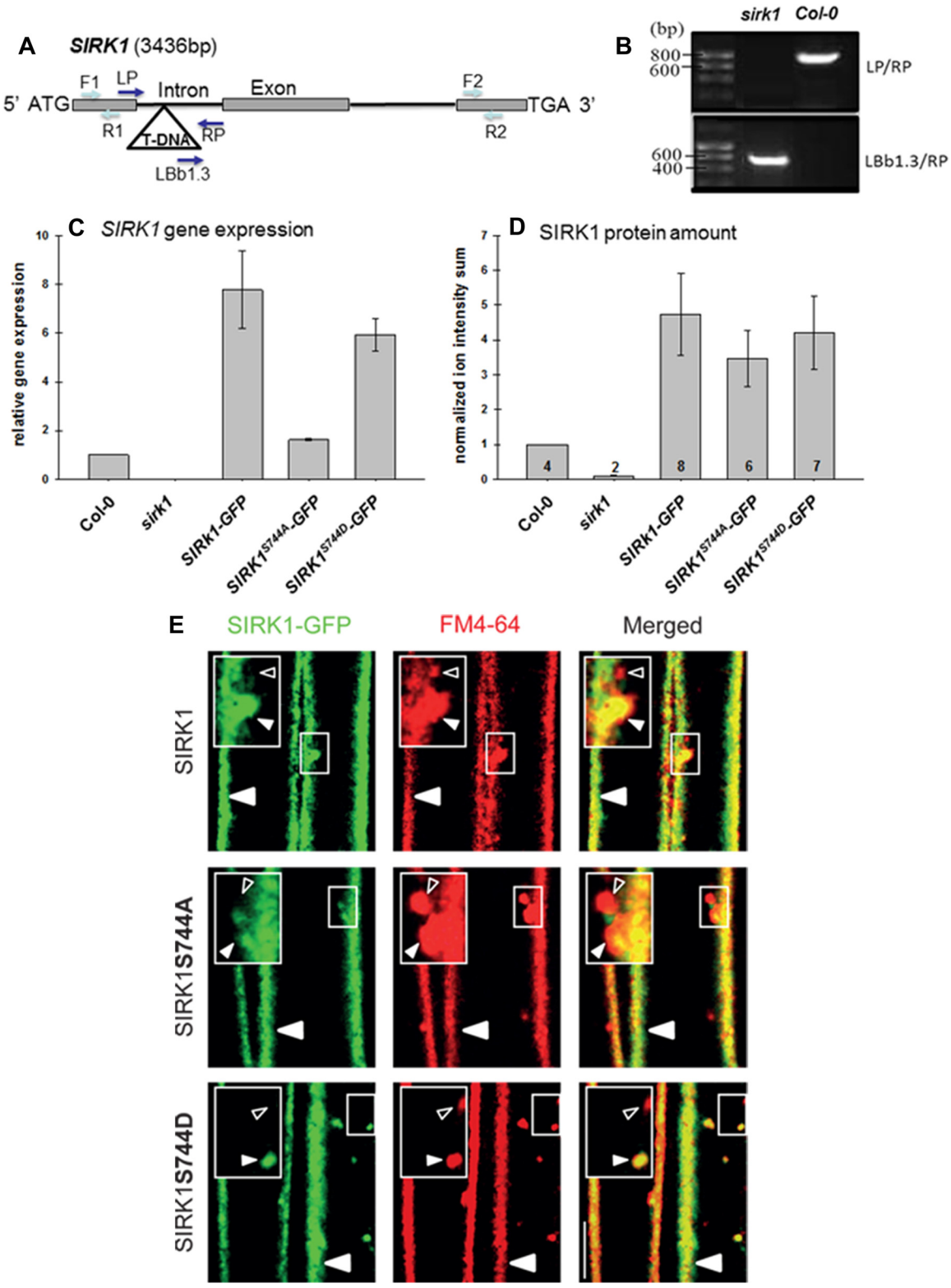

FIG. 1. **Identification of a T-DNA insertional mutant of SIRK1.** *A*, *SIRK1* gene structure with T-DNA insertion in the first intron. *B*, confirmation of the T-DNA insertion in homozygous progeny of *sirk1*. *C*, expression of *SIRK1* was tested by quantitative real-time PCR in wild-type, T-DNA insertional mutant, and *SIRK1* overexpression and *SIRK1* mutagenesis lines in *sirk1* background. The relative expression of three biological replicates (average ± standard deviation) is displayed in comparison to the wild type, which was set to 1. *D*, normalized ion intensity of SIRK1 peptides identified in plasma membrane purifications before phosphopeptide enrichment. Ion intensity sum fractions of total

but ion intensities for two peptides, FSDQPVMLDVYSPDR and NEIWGDVGEIFTELK, were assigned based on retention-time correlation. In general, peptide ion intensity sums for SIRK1 in the T-DNA insertional mutant were at least 10 times lower than in the wild type (Fig. 1*D*). For complementation of *sirk1* mutants, the *SIRK1* cDNA was cloned as a GFP fusion and expressed under the CaMV35S promoter, resulting in higher expression of *SIRK1* relative to the wild type (Fig. 1*C*). Furthermore, *SIRK1-GFP*-fusion constructs were made for *SIRK1*, in which the serine 744 was mutated to either alanine (S744A) or aspartic acid (S744D) to result in phosphorylation site null mutants and phosphorylation mimics. Relative expression levels of the phosphorylation site mutant constructs were similar to those observed for the native construct (Fig. 1*C*). Predicted SIRK1 localization to the plasma membrane was confirmed by confocal imaging of the GFP-fusion constructs in overlay images with membrane staining dye FM4-64 (Fig. 1*D*). The localization of SIRK1 in the plasma membrane was not altered by the mutations on S744; all three SIRK1 constructs (SIRK1-GFP, SIRK1^{S744A}-GFP, and SIRK1^{S744D}-GFP) localized at the plasma membrane and to endosomes (zoom-in boxes in Fig. 1) overlapping with FM4-64 (solid triangles in Fig. 1).

SIRK1 Is an Active Kinase—SIRK1 and the phosphorylation site mutants showed kinase activity when exposed to a generic substrate, such as myelin basic protein, as recorded by reduced luminescence in a luciferase-dependent measurement of residual ATP in the assay (Fig. 2) (high luminescence correlates with low phosphorylation). The kinase activity of SIRK1 isolated from microsomal fractions of *sirk1* seedlings expressing the *^{35}S::SIRK1-GFP* construct was significantly increased upon sucrose resupply after sucrose starvation. In contrast, for *sirk1* mutants expressing *^{35}S::GFP* only (empty vector control (EVC)), kinase activity in sucrose-starved and sucrose-resupplied seedlings remained unaltered. In general, kinase activity in plants expressing GFP only was significantly lower even relative to sucrose-starved *sirk1* plants expressing the *^{35}S::SIRK1-GFP* or the site directed mutant constructs *^{35}S::SIRK1^{S744A}-GFP* and *^{35}S::SIRK1^{S744D}-GFP*. Mutation of the SIRK1 phosphorylation site at serine 744 to alanine resulted in kinase activity similar to that of sucrose-starved *^{35}S::SIRK1-GFP* plants, and kinase activity did not significantly increase upon sucrose exposure. In contrast, when serine 744 was mutated to aspartic acid, subsequent kinase activity was more similar to that of the sucrose-induced *^{35}S::SIRK1-GFP* plants and remained higher under sucrose starvation. In all cases, although SIRK1 protein was isolated from different plant lines, the amount of SIRK1 protein present

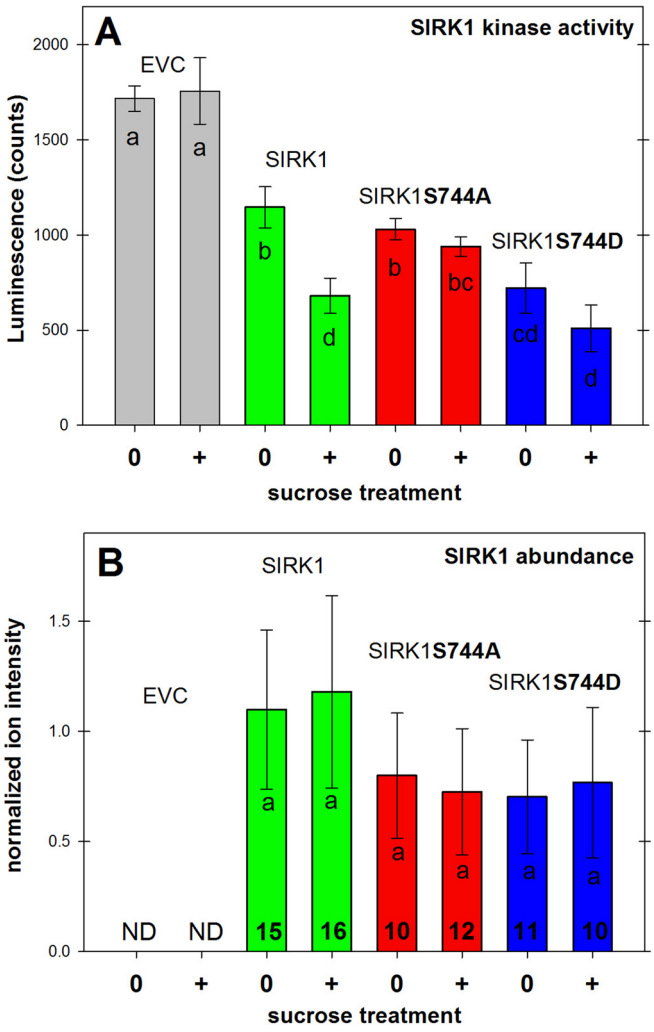

FIG. 2. **Kinase activity of SIRK1 and its site-directed mutants SIRK1^{S744A} and SIRK1^{S744D} using a luciferase-based luminescence assay.** *A*, myelin basic protein was used as a generic kinase substrate. Seedlings of *sirk1* expressing the different SIRK1-GFP fusion constructs were starved for sucrose over 24 h and then resupplied with sucrose for 3 min before protein extraction and pull-down of GFP-tagged SIRK1. High luminescence values correlate to high ATP concentrations, meaning low phosphorylation. *B*, normalized ion intensity sums of peptides identified for SIRK1 in the pull-downs subjected to the kinase activity assay and analysis of interaction partners. Numbers within the bars indicate the number of SIRK1 peptides identified. Averages with standard deviations of three biological replicates are displayed. Small letters indicate significant differences between different treatments as determined via one-way analysis of variance and pairwise multiple comparison procedures according to Holm-Sidak ($p < 0.05$). EVC: empty vector control, expressing GFP only. ND: not detectable.

ion intensity in each sample were averaged and expressed relative to col-0 wild type. Numbers within the column indicate the numbers of different peptide species identified. *E*, SIRK1, SIRK1S744A, and SIRK1S744D localize at the plasma membrane and in endocytotic structures (solid triangles in zoom-in boxes) as shown in confocal images of sucrose-starved four-day-old etiolated hypocotyl cells of ^{35}S::SIRK1-GFP, ^{35}S::SIRK1^{S744A}-GFP, and ^{35}S::SIRK1^{S744D}-GFP lines. Seedlings expressing SIRK1-GFP, phospho-null-GFP (SIR1**S744A**), and phospho-mimic-GFP (SIRK**S744D**) were incubated in 20 μM FM4-64 for 10 min. FM4-64 also stains endosomes, which do not contain the corresponding SIRK1 construct (open triangles in zoom-in boxes). Scale bar = 20 μm.

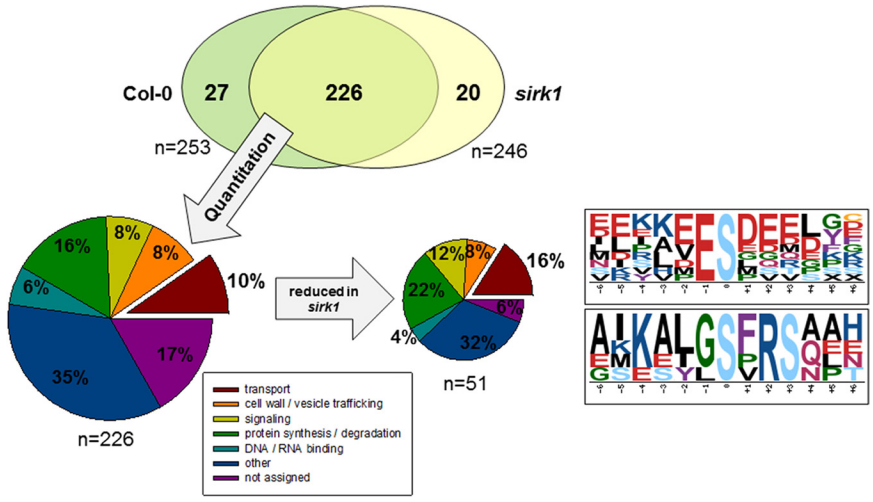

FIG. 3. **Three minutes of sucrose treatment on sucrose-starved seedlings for col-0 and *sirk1* mutant revealed a total of 226 commonly quantified phosphopeptides.** Significantly altered sucrose-induced phosphorylation was observed for 68 peptides. In particular, the phosphorylation of transport proteins ($p = 8 \times 10^{-6}$, Fisher's exact test) was reduced in *sirk1*. Two phosphorylation motifs were identified among the differentially phosphorylated peptides.

in the assay was not significantly different for different constructs (Fig. 2*B*).

Identification of Putative SIRK1 Targets via Phosphorylation Profiling in Sucrose-induced Conditions—In order to study the role of SIRK1 in the context of rapid alterations in external sucrose availability, a sucrose starvation and resupply experiment was carried out with seedlings of wild type and *sirk1* mutant. Sucrose was resupplied to carbon-starved seedlings to a final concentration of 30 mM for 3 min. This was the time point at which maximal transient phosphorylation of SIRK1 had been observed in previous work (43). In total, 369 phosphopeptides were identified in at least one genotype or condition. Spectra for all identified phosphopeptides were submitted to the phosphorylation site database PhosPhAt and also can be found in supplemental Fig. S1. From these, 253 phosphopeptides were quantified in wild type both in starved seedlings and after 3 min of sucrose resupply; for the *sirk1* mutant, 246 phosphopeptides were quantified under both conditions. This resulted in an overlapping 226 phosphorylation sites with quantitative information for both time points in wild-type and *sirk1* mutant seedlings (Fig. 3). To identify significant alterations in sucrose-induced phosphorylation between the wild type and the *sirk1* mutant, the variation in sucrose-induced phosphorylation as calculated from phosphopeptide ion intensity ratios of the sucrose-induced state relative to the sucrose-starved state was analyzed within the replicates of each plant line (comparisons of col-0 *versus* col-0 or *sirk1 versus sirk1*). In contrast, comparison of the sucrose-induced phosphorylation ratios between *sirk1* and col-0 revealed a significantly different distribution of sucrose-induced phosphorylation ($p = 0.013$, Kolmogorov-Smirnov test; supplemental Fig. S2). Particularly, for *sirk1* in comparison to wild type, the distribution of sucrose-induced phosphorylation ratios ($\log_2$(3 min sucrose/sucrose starved)) was shifted to lower ratios, suggesting that protein phosphorylation in *sirk1* did not increase in response to the sucrose stimulus to the same degree as in wild-type col-0.

In detail, about 30% of all 226 quantified phosphopeptides showed an altered abundance in *sirk1* mutant relative to the wild type, with 51 phosphopeptides displaying at least 2-fold lower sucrose-induced phosphorylation and 19 phosphopeptides showing at least 2-fold higher sucrose-induced phosphorylation relative to the wild type (supplemental Table S3). We could confirm the sucrose-induced phosphorylation of the SIRK1 peptide FSDQPV(oxM)LDVY(pS)PDR bearing S744 (43). Sucrose-induced phosphorylation of this peptide was abolished in *sirk1* mutant and partially restored in the SIRK1-GFP overexpression line (supplemental Fig. S3).

In general, proteins with transport functions (aquaporins, SWEET11, ATPases) were overrepresented ($p = 8 \times 10^{-6}$, Fisher's exact test, using all identified proteins as a background; Fig. 3) among phosphopeptides with reduced sucrose-induced phosphorylation in *sirk1*, followed by proteins with functions in protein synthesis ($p = 0.0007015$, Fisher's exact test). Peptides of transport-related proteins were the Ca^{2+} ATPase ACA8 (AT5G57110), the sucrose exporter SWEET11 (AT3G48740), the vacuolar glucose exporter ERDL6 (AT1G75220), and, particularly, peptides originating from the C-terminal end of different aquaporins (PIP3A AT4G35100, PIP2E AT2G39010, PIP2B AT2G37170, PIP2F AT5G60660). For signaling proteins, the sucrose-induced phosphorylation of protein kinase SnRK2.5 (AT5G63650.1) phosphopeptide IFV(pT)NSAKR was found to be reduced in *sirk1*. Other signaling proteins with reduced phosphorylation in *sirk1* included FHL (AT5G02200), NPH3 (AT5G64330), the Rab protein ARA4 (AT2G43130), and a remorin family protein (AT3G61260). Furthermore, for seven ribosomal proteins and one translation initiation factor, protein phosphorylation in response to external sucrose was reduced in *sirk1*. For another 14 proteins, SIRK1 overexpressing lines showed increased sucrose-induced phosphorylation that remained unaltered in *sirk1*. For example, the sucrose-induced phosphorylation of NSLNI(pS)MR of kinase CPK5 (AT4G35310) was only slightly reduced in *sirk1*, but it showed a higher phosphorylation state in SIRK1 overex-

pressing lines than in wild-type seedlings after sucrose-induced phosphorylation.

The phosphopeptides identified with reduced sucrose-induced phosphorylation contained two significant ($p < 0.01$) phosphorylation motifs (67): an ES motif (motif score = 3.17) that was mainly found in the ribosomal proteins, and an SXRS motif (motif score = 6.93) that particularly contained the double-phosphorylation sites of the aquaporin peptides (Fig. 3). A search for the SXRS motif in the PhosPhAt database (44) revealed a total of 69 phosphopeptide sequences, and phosphorylation was shown for 33% of these for both serine residues. The SXRS motif thus seems to be a double-phosphorylation site motif, and possibly the same kinase can address both sites.

For 19 proteins, higher sucrose-induced phosphorylation was observed in the *sirk1* T-DNA insertional mutant. Among them we found enzymes of central carbon and nitrogen metabolism, such as sucrose phosphate synthase SPS1F (AT5G20280), an isoform of cytosolic glutamine synthase GLN1;1 (AT5G37600), glutamate decarboxylase GAD1 (AT5G17330), and asparagine synthase ASN2 (AT5G65010). The phosphorylation site in peptide IN(pS)AESMELWASQQK of sucrose phosphate synthase SPS1F was found to be the major regulatory phosphorylation site, leading to inactivation of the enzyme in phosphorylated status (6). Observations of levels of sucrose-induced phosphorylation of these proteins higher than found in the wild type might point to the involvement of additional proteins, such as protein kinases or phosphatases that are inactivated or activated by SIRK1.

For 33 phosphopeptides of the 51 proteins with decreased phosphorylation in *sirk1*, a trend or significant increase of sucrose-induced phosphorylation was observed in the *^{35}S::SIRK1-GFP* overexpression line relative to the *sirk1* mutant. For most of these phosphopeptides, sucrose-induced phosphorylation reached levels similar to those in wild-type plants (supplemental Table S3).

The major apparent phosphorylation targets of SIRK1, namely, aquaporin proteins, were confirmed by an *in vitro* phosphorylation assay involving synthetic peptides. An *in vitro* kinase assay was performed using a mixture of 43 different peptides as a substrate. The peptide mixture contained a total of 25 peptides matching various experimentally confirmed phosphorylation sites, including the C-terminal peptide ALGSFGSFGSFR of aquaporin PIP2F (AT5G60660), LGTVSSPEPISVVR from SWEET11 (AT3G48740), and peptide LIEEVSHSSGSPNPVSD of receptor kinase AT3G02880. In addition, 18 control peptides were included, one for each of the putative substrate proteins. After exposure to SIRK1, only peptides ALGSFGSFGSFR, LGTVSSPEPISVVR, and LIEEVSHSSGSPNPVSD were found to be phosphorylated, whereas 14 other peptides with experimentally confirmed phosphorylation sites were detected in the non-phosphorylated form. For peptide ALGSFGSFGSFR, the singly phosphorylated versions ALGSFG(pS)FGSFR and ALGSFGSFG(pS)FR and the doubly phosphorylated version ALGSFG(pS)FG(pS)FR were detected. Quantitative analysis of the PIP2F phosphopeptides revealed increased phosphorylation of peptide ALGSFGSFGSFR at two different phosphorylation sites upon exposure to the SIRK1-GFP constructs relative to GFP-only purifications (EVC). The phosphorylation of PIP2F substrate peptide was independent of phosphorylation site mutagenesis (supplemental Fig. S4). The control peptide for PIP2F, with no phosphorylation sites (DPPPAPFFDMEELR), did not show altered ion intensity levels after exposure to the SIRK1 variants. Altogether, 8 putative target peptides (from total of 25) and 5 control peptides (from total of 18) were not detected in the mass spectrometric analysis after *in vitro* kinase exposure. For technical reasons, the peptide ALGSFGSFGSFR was the only C-terminal aquaporin peptide included in the *in vitro* assay; related peptides SLGSFR(pS)AANV (PIP2B), ALGSFR(pS)NATN (PIP3), and (pS)QLHELHA (PIP2E) were not tested in this context.

Sucrose-induced Interaction Partners of SIRK1—We were interested in sucrose-induced protein–protein interaction partners of SIRK1. Therefore, GFP pull-downs under sucrose-starvation conditions (time point: 0 min) and under sucrose-resupplied conditions (time point: 3 min) were performed with *sirk1* seedlings expressing the different SIRK1-fusion proteins or GFP only (EVC). Under each sucrose treatment condition (starvation or resupply), protein ion intensity sums of interaction partners for each of the bait GFP-fusions (SIRK1, SIRK1^{S744A}, and SIRK1^{S744D}) were expressed relative to the interaction partners of the GFP-only control (EVC) under that condition. Results from three biological replicates were averaged and significant interaction partners were defined after pairwise *t* test and multiple-testing correction (64). The full list of all 1386 identified proteins in the pull-down experiments of the different bait protein versions is available as supplemental Table S2, and the full results of pairwise *t* tests of bait *versus* GFP-only samples, including corrected and uncorrected *p* values, are available as supplemental Table S4.

In pull-downs with SIRK1 bait proteins, under sucrose-induced conditions (3 min sucrose supply), two to three times more proteins were identified as significant interaction partners ($p < 0.05$ after multiple testing correction) than in the sucrose-starved condition, although SIRK1 bait was present in similar amounts (Fig. 2*B*). A large overlap in identified proteins was observed for the three SIRK1 constructs (SIRK1-GFP, SIRK1^{S744A}-GFP, and SIRK1^{S744D}-GFP), with a tendency for stronger overlap between SIRK1 and SIRK1^{S744A} than between SIRK1 and SIRK1^{S744D} (Fig. 4*A*). Among the significant interaction partners ($p < 0.05$ after multiple testing correction) were also numerous ribosomal proteins and proteins with plastidal locations. These protein classes are known to be particularly "sticky" and often occur as nonspecific interactors in pull-downs. Therefore, only proteins with plasma membrane or extracellular locations based on the consensus location from SUBA3 were considered (66). A total

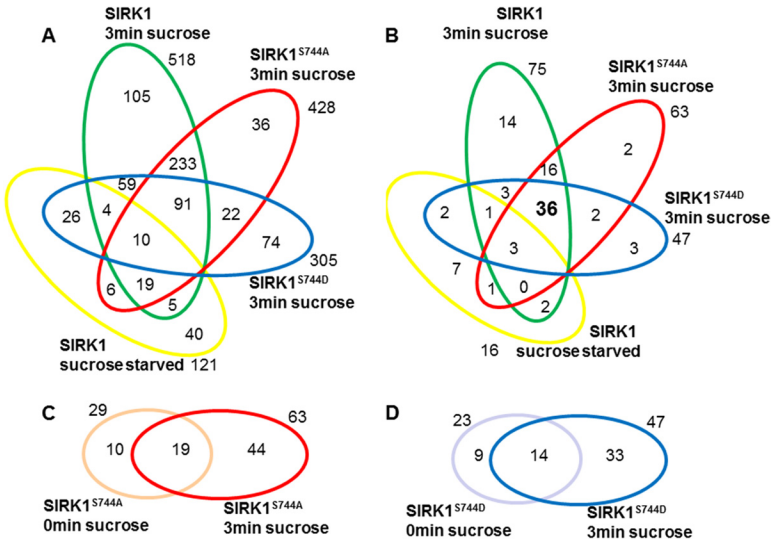

FIG. 4. **Conditional interaction partners to SIRK1 and SIRK1-S744 mutants.** *A*, all identified proteins from pull-downs and with significantly higher abundance in the bait pull-down relative to the respective GFP-only controls are shown for the various baits and conditions. *B*, interaction partners were filtered for plasma membrane or extracellular location. *C*, interaction partners to SIRK1^{S744A} in sucrose-starved and sucrose-resupplied condition. *D*, interaction partners to SIRK1^{S744D} in sucrose-starved and sucrose-resupplied condition. In general, only significant interactors are shown ($p < 0.05$ in pairwise *t* test of each proteins from comparison of bait pull-down to GFP-only pull-down and after multiple-testing correction according to Benjamini-Hochberg (64)).

of 36 proteins remained as significant sucrose-induced interaction partners for all SIRK1 constructs (Fig. 4*B*). Among these common interactors, we found a strong overrepresentation ($p = 4.53 \times 10^{-10}$, Fisher's exact test) of aquaporins, particularly PIP1A (AT3G61430), PIP1C (AT1G01620), PIP2A (AT3G53420), PIP2B (AT2G45960), PIP1D (AT4G23400), PIP2E (AT2G39010), PIP2F (AT5G60660), and PIP3A (AT4G35100). Other significant interaction partners to SIRK1 and its site-directed mutants were a number of protein kinases, such as three transmembrane-receptor-like protein kinases, as well as two kinases from the BSK family (Table I). The BSK kinases were shown to be involved in the brassinosteroid signaling pathway initiated by receptor kinase BRI1 (68). Other significant interaction partners to SIRK1 were clathrins (AT2G20760, AT3G08530, AT3G11130) and a coatomer subunit protein (AT4G31480) indicating connections to endocytotic pathways. Interestingly, members of the remorin family of proteins were identified exclusively under sucrose-resupplied conditions, with more than 2-fold enrichment in the different SIRK1 pull-downs relative to GFP only. Remorins are proteins with clear preferable location in sterol-rich membrane microdomains (69, 70).

SIRK1 Modulates Water Flux across the Plasma Membrane—In the phosphopeptide profiling experiment comparing sucrose-induced phosphorylation of wild type and *sirk1*, several phosphopeptides matching the C-terminal end of aquaporins were identified, and aquaporins were found as interaction partners of SIRK1. Thus, we hypothesized that SIRK1, either independently or within a complex of interacting proteins, may be involved in the regulation of aquaporin activity, particularly given that aquaporins are known to be regulated by protein phosphorylation. The identified differentially phosphorylated sites in wild-type and *sirk1* mutant samples at the C terminus of aquaporins are conserved in the aquaporin protein family and are responsible for pore gating. Full phosphorylation at the two serine residues will lead to pore opening, whereas dephosphorylated serine residues result in a closed pore (31). Therefore, the water transport capacity of wild type, *sirk1* mutant, and the different lines expressing SIRK1 and S744 mutants were analyzed in a protoplast swelling assay reflecting the aquaporin activity (30).

When exposed to a hypo-osmolar medium, protoplasts take up water through aquaporins; this can be observed in the swelling of the protoplasts (Fig. 5*A*). Protoplasts were prepared from sucrose-starved seedlings and initially exposed to 500 mM mannitol (approximately 580 mOsmol kg^{-1}). Then, the protoplasts were challenged either with 350 mM mannitol or with 320 mM mannitol containing 30 mM sucrose (approximately 400 mOsmol kg^{-1} for both media). The water flux density (j_v) across the protoplast membrane was calculated from video records of individual protoplasts. In the wild type, sucrose-containing medium induced a higher ($p = 0.021$) swelling rate than mannitol medium alone (Fig. 5*B*). This was completely abolished in the *sirk1* mutant, which showed significantly less swelling ($p < 0.001$) upon sucrose treatment than upon mannitol treatment. In the complementation line expressing *^{35}S::SIRK1-GFP*, the significant increase ($p = 0.002$) in water flux density upon sucrose treatment was restored (Fig. 5*C*). The higher water flux density in the complementation line than in the wild-type sucrose-induced protoplasts might be due to overexpression of SIRK1 under the CaMV35S promoter. There were no significant differences in water flux densities among wild-type, *sirk1*, and SIRK1 expressing lines when treated with mannitol only. The mutation of S744 to alanine or aspartic acid did not result in a significantly different water flux density in mannitol medium. Protoplasts from the two site-directed mutant lines also showed increases in water flux densities similar to those in plants expressing wild-type SIRK1. In general, the mutants of SIRK S744 were still able to phosphorylate aquaporins (supplemental Fig. S5), indicating that mutations at S744 did not affect kinase activity.

TABLE I

Results of the protein–protein interaction studies using GFP-fusions of SIRK1, SIRK1^{S744A}, and SIRK1^{S744D} as bait under either sucrose-starvation conditions or sucrose-resupplied conditions for 3 min. Numbers indicate the protein abundance ratio of bait pull-down to GFP-only control and were obtained by averaging results from three biological replicates. Asterisks indicate significant differences ($p < 0.05$) after pairwise t tests of normalized ion intensity sums for bait pull-down versus control pull-down and after multiple-testing correction (64). The minimum p value across all conditions is shown; individual p values and standard deviations for the displayed averaged ratios are available in supplementary Table S4

Interactor	Normalized ion intensity sums log2(bait/GFP-only)						Description	Minimum *p* value (*t* test)
	Sucrose starvation			Sucrose resupply (3 min)				
	SIRK1	SIRK1^{S744D}	SIRK1^{S744A}	SIRK1	SIRK1^{S744D}	SIRK1^{S744A}		
Aquaporins								
AT1G01620	0.689			**2.008***	**1.113***	**1.492***	PIP1C, PIP1;3	1.56E-06
AT2G37170				1.553		1.359	PIP2B, PIP2;2	0.052843
AT2G39010		0.761*		**1.599***	**1.293***	**1.540***	PIP2E, PIP2;6	5.29E-05
AT3G53420				**2.038***	0.840*	**1.313***	PIP2A, PIP2;1	1.29E-15
AT3G61430				**2.027***	**1.152***	**1.449***	PIP1A, PIP1;1	9.26E-07
AT4G00430						2.678	PIP1E, PIP1;4	0.087501
AT4G23400	0.721	0.692		**1.965***	**1.298***	**1.126***	PIP1D, PIP1;5	0.000336
AT4G35100				**1.979***	**1.119***	**1.434***	PIP3A, PIP2;7	1.1E-13
AT5G60660			−0.736	**1.578***	1.817	2.338	PIP2F, PIP2;4	0.040114
Kinases								
AT2G43230	**2.075**						Protein kinase superfamily protein	0.051732
AT3G02880			−0.770	**1.358***		1.063	Leucine-rich repeat receptor-like protein kinase	0.040978
AT3G14840				1.249		1.406	Leucine-rich repeat receptor-like protein kinase	0.078647
AT3G63260				2.506			RAF-kinase ATMRK1	0.078331
AT4G08850			−1.511	1.830	2.291		Leucine-rich repeat receptor-like protein kinase	0.084065
AT4G35230				**1.479***	1.568	1.088	BSK1 (BR-signaling kinase 1)	0.025121
AT5G46570						1.701	BSK2 (BR-signaling kinase 2)	0.064452
Remorins								
AT2G45820				1.078			Remorin family protein	0.076945
AT3G61260	0.544			**1.537***	**1.165***	**1.074***	Remorin family protein	1.80E-06
Clathrins and coatomers								
AT2G20760		**1.198***		0.893*	**1.065***	0.868*	Clathrin light chain protein	0.005237
AT3G08530		**1.039***	−0.855*	0.979*		0.782*	Clathrin, heavy chain	0.000711
AT3G11130		**0.887***	−0.688*	0.946*	0.506*	0.631*	Clathrin, heavy chain	3.08E-43
AT4G31480			−0.745*	**1.217***	0.700*	0.750*	Coatomer beta subunit	2.85E-08
Other								
AT2G45470				0.935*	0.511	0.701*	FLA8	0.000804
AT1G03870				0.741*		0.623*	FLA9	0.007464
AT2G20990			**−1.241***	**1.440***		0.997*	SYTA, synaptogamin A	1.43E-06
AT1G16890				**2.117***	**1.500***	**1.784***	UBC36, ubiquitin conjugating enzyme 36	2.47E-05
AT1G72150	0.748*	**1.096***		**1.686***	**1.666***	**1.680***	PATL1, Patellin1	2.78E-45
AT1G22530	0.766*	**1.063***	0.555*	**1.138***	**1.121***	**1.085***	PATL2, Patellin2	1.18E-20
AT1G41830		**1.131***		**1.942***	**1.415***		SKS6	0.016744
AT4G20260		**1.023***		**1.670***	**1.363***	**1.390***	PCAP1	4.80E-24
AT1G54000		0.515*		0.523*	0.946*	0.684*	GDSL-like lipase	1.32E-09
AT1G54010		0.586*		0.774*	**1.176***	0.994*	GDSL-like lipase	2.04E-16
AT1G78830		**1.264***	0.723*	**1.378***	**1.895***	**2.167***	Cucurlin-like lectin family protein	2.49E-07
AT1G78850		**1.376***	0.956*	**1.551***	**2.001***	**1.965***	D-mannose binding lectin family protein	3.21E-10
AT4G35790			−1.280	**1.376***	0.946	**1.295***	PLD delta, phospholipase D	0.001986

Role of S744 in Sucrose-induced Responses—In order to gain insights into the role of serine 744 phosphorylation sites in sucrose-related responses, we also performed sucrose-starvation experiments followed by 3 min of sucrose resupply using the *sirk1* mutants expressing either S744A or S744D mutants of SIRK1 (SIRK^{S744A} and SIRK^{S744D}). We assumed that an aspartic acid (D) substitution mimics a constitutive phosphorylation of Ser-744, and that alanine (A) produces a phosphorylation-null mutation. There was a slight trend for the plants expressing SIRK1^{S744D} showing more wild-type-like sucrose-induced phosphorylation of aquaporin PIP2E (AT2G39010) (supplemental Fig. S5) or other proteins, such as tonoplast located ERDL6 (AT1G75220). This trend was supported by our findings of slightly higher kinase activity in SIRK1^{S744D} than in SIRK1^{S744A} (Fig. 2).

The results from SIRK1 pull-downs indicated 16 significant interaction partners ($p < 0.05$) as more frequent interactors to SIRK1^{S744A} than to SIRK1^{S744D} (Fig. 4*B*) based on pairwise significance testing of abundance ratios relative to the GFP-only control. Among these proteins were FASCICLIN-like arabinogalactan proteins (AT2G45470, AT1G03870), synamptogamin A (AT2G20990), a ubiquitin-conjugating enzyme (AT1G16890),

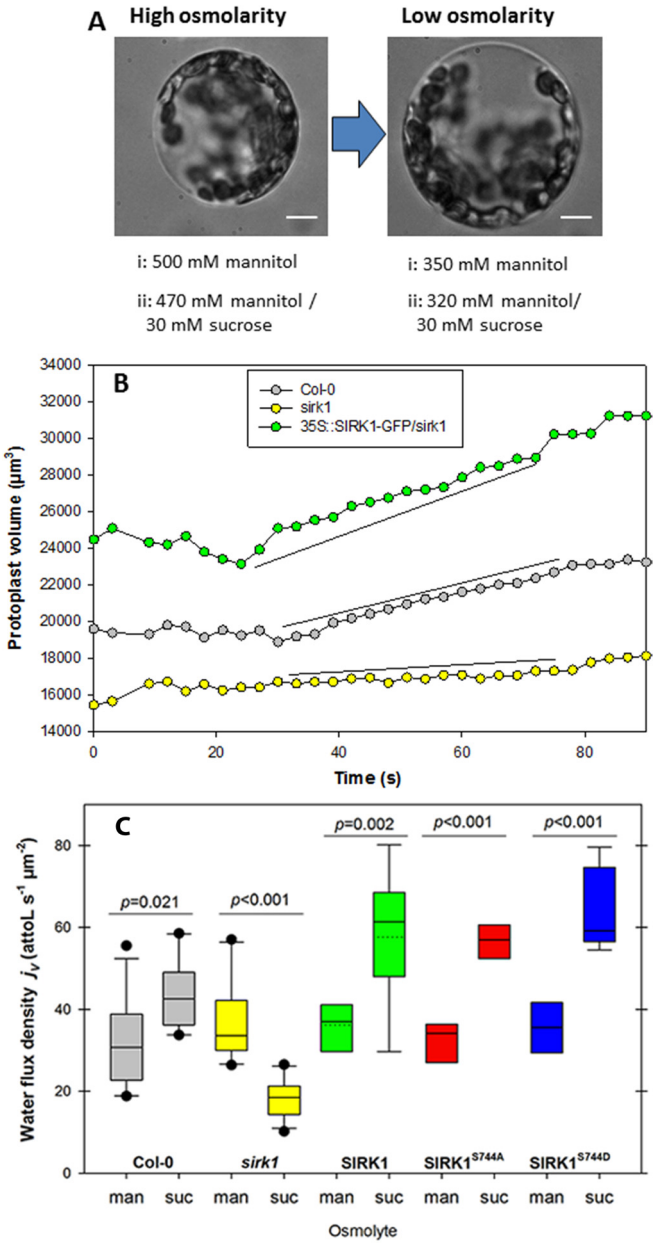

FIG. 5. **Protoplast swelling assay.** *A*, protoplasts from sucrose-starved seedlings were exposed to a low-osmolarity mannitol- or sucrose-containing medium, and swelling was recorded by mean sof video microscopy. *B*, examples of protoplast volume over time after challenge with low-osmolarity medium. The slope of the curves was used to calculate the volume flux density. *C*, boxplots of water flux densities (j_v) from up to 12 individual protoplasts per treatment for mannitol (man) and sucrose (suc) as an osmolyte. *p* values indicate significant differences between mannitol and sucrose treatments within each plant line. Significance between treatments was tested by pairwise *t* test. bar = 5 μm.

and a phospholipase D (AT4G35790) (Table I). Among the 223 proteins found as common interaction partners to SIRK1 and SIRK1^{S744A} (Fig. 4*A*), we found four members of the thioredoxin family (AT1G45145, AT4G03520, AT5G39950, and AT5G42980), six 14–3-3 proteins (AT1G78300, AT2G42590, AT4G09000, AT5G10450, AT5G38480, and AT5G65430), six proteins with functions in G-protein signaling (AT1G16920, AT1G56330, AT3G18820, AT4G17170, AT5G20010, and AT5G59840), and seven isoforms of tubulin (AT1G04820, AT1G20010, AT4G-14960, AT5G12250, AT5G19770, AT5G62690, and AT5G44340). Among the membrane-located interaction partners to SIRK1^{S744A}, synaptogamin A (AT2G20990), sugar transporter STP1 (AT1G11260), and plasma membrane ATPase AHA2 (AT4G30190) were found with abundance ratios that were higher in the sucrose-supplied status (supplemental Table S4, Fig. 4*C*).

In contrast, 14 proteins with membrane or external locations were identified as significant interaction partners to SIRK1^{S744D} independent of the sucrose status (Fig. 4*D*). This constituted 29% of all 47 identified membrane-located significant interaction partners of SIRK1^{S744D}. Among these sucrose-independent interactors were aquaporin PIP2E (AT2G39010), as well as proteins with functions in membrane trafficking, cell wall or membrane microdomains (*e.g.* PATL1 (AT1G72150) and PATL2 (AT1G22530) or SKS6 (AT1G41830)), and three clathrins (AT2G20760, AT3G08530, and AT3G11130). PCAP1 (AT4G20260) related to phosphoinosite signaling (four proteins: AT1G5400, AT1G54010, AT1G78830, and AT1G78850) belonged to the MAPMAN category "myrosinases-lectin-jacalin." All of these proteins were also identified as significant interaction partners to SIRK1 with a non-mutated phosphorylation site, but only in the sucrose-induced state (Table I). These findings might be indicative of a role of S744 phosphorylation in either protein targeting or sucrose-induced internalization of SIRK1. Because interactions with proteins with functions in receptor internalization or trafficking were found to be stronger in the S744D mutant, we propose that phosphorylation at S744 might be one way to induce the rapid internalization of SIRK1 and thus lead to adjustment of receptor availability during or after stimulation.

A role of S744 phosphorylation in connection with receptor internalization was confirmed through the observation of SIRK1 accumulation in sucrose-induced endocytotic events. Clearly, sucrose stimulation for up to 15 min induced the formation of endosome-like structures containing SIRK1 in SIRK1-GFP overexpressing plants (Fig. 6). If S744 was mutated to a phosphorylation-null mimic (S744A), the frequency of SIRK1 endocytosis was significantly reduced, as shown by the less frequent observation of cells with many sucrose-induced SIRK1-containing endocytotic vesicles. In contrast, if S744 was mutated to a constitutive phosphorylation mimic (S744D), the number of cells with few SIRK1-containing endocytotic events in the absence of sucrose was strongly increased (Fig. 6). Interestingly, in this mutant, the number of cells with many SIRK1-containing endocytotic events under non-induced conditions was slightly higher than observed in the wild-type version. Interestingly, the S744D mutant did not respond to sucrose resupply. Thus, some degree of phosphory-

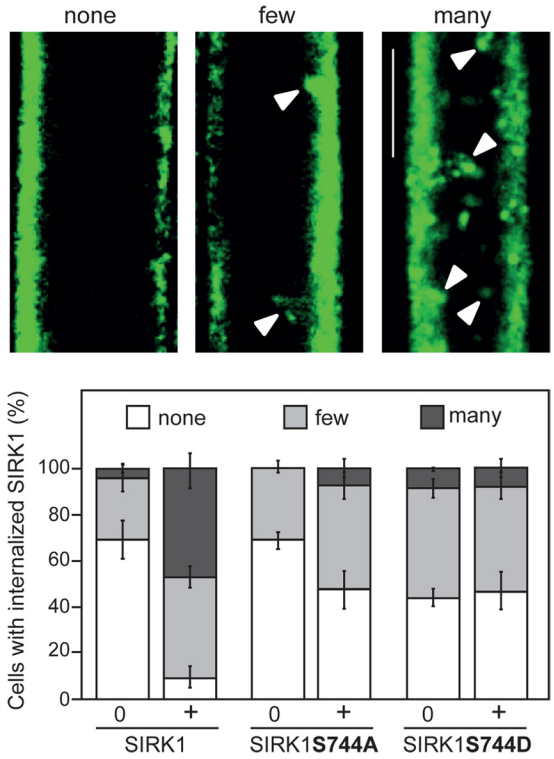

FIG. 6. **SIRK1 overaccumulates in endocytic events after sucrose resupply.** This response to sucrose is altered in the phospho-null (SIRK1^{S744A}) and phospho-mimic (SIRK1^{S744D}) constructs. The percentage of hypocotyl cells displaying no detectable (white), few (light gray), or many (dark gray) SIRK1-GFP endocytic events is presented. Seedlings expressing SIRK1-GFP, phospho-null-GFP (SIR1^{S744A}), and phospho-mimic-GFP (SIRK^{S744D}) were imaged without (0) and with (+) sucrose resupply for 3 to 15 min. Data represent the average (± S.E.) of at least eight seedlings and 20 cells per seedling counted by genotype and treatment. Confocal images of four-day-old etiolated hypocotyl cells of ^{35}S::SIRK1-GFP are shown as a reference. Solid triangles indicate endosomal structures. Scale bar = 20 μm.

lation at S744 resulted in increased SIRK1 endocytosis relative to the non-phosphorylated condition (S744A).

DISCUSSION

The transmembrane receptor kinase family is the largest protein kinase family in Arabidopsis (71) and the kinase family with the largest fraction of proteins with yet uncharacterized functions. Prominent and well-characterized members of the receptor kinase family are the brassinosteroid receptor BRI1 (72), the flagellin receptor FLS2 (73), and CLAVATA1, a receptor for the peptide CLAVATA3 (74). Other members of the receptor kinase family are also involved in the perception of peptide hormones (75) or other growth-promoting substances (76). Receptor kinases are known to be phosphorylated in a stimulus-dependent manner, as discovered in various comparative phosphoproteomics experiments (37, 42, 77, 78). Under the assumption that transient stimulus-dependent phosphorylation indicates functional roles under the respective conditions, SIRK1 was identified as potentially involved in sucrose-induced signaling processes (43). The present study aimed at gaining functional insights into the role of SIRK1 in sucrose-induced responses.

Use of Kinase Mutants for the Identification of Putative Substrates—In mammalian systems, systematic studies for the identification of kinase substrates have been carried out using ATP-analog-sensitive kinase mutants (79, 80). This approach was also followed in QIKS (the quantitative identification of kinase substrates), which was used to identify cytoplasmic substrates of the MAP-kinase MEK1 by incubating protein extracts of mek1 cells with recombinant mutated MEK1, which takes an ATP analog as a substrate (81). Other proteomic approaches in studying protein kinase functions include the use of specific kinase inhibitors (82) or kinase-selective enrichment methods (83). However, in our case, these latter strategies were not readily applicable because of insufficient knowledge of specific kinase inhibitors or binding proteins for SIRK1.

Therefore, we used an unbiased approach of phosphopeptide profiling to identify possible target proteins of receptor kinase SIRK1. It was assumed that in a *sirk1* expression mutant, the same stimulus (in our case, sucrose) would result in reduced protein phosphorylation of SIRK1 substrate proteins. This approach also assumed that other kinases with similar functions would not completely take over SIRK1 functions and phosphorylation patterns. For mammalian receptor tyrosine kinases, it was described that different kinases can actually phosphorylate the same target proteins but differ in their quantitative degree of phosphorylation (84). A large-scale and systematic comparative analysis of protein phosphorylation patterns in wild-type and kinase- or phosphatase-deletion mutants of yeast (85) revealed specific phosphorylation patterns for 78% of the kinases analyzed. However, a high degree of robustness and interconnectivity in signaling pathways was concluded from lacking or mild growth phenotypes for most of the kinase/phosphatase deletions. Thus, although the identification of kinase substrates merely based on the absence of identified phosphopeptides is likely to be very difficult, the characterization of putative kinase targets based on the quantitation of phosphorylation levels was found to be quite successful. Thus, enrichment of the compartment of interest—such as, for instance, membrane proteins—will improve the chance of finding relevant proteins.

SIRK1 as a Membrane-bound Kinase Directly Regulates Transport Processes—Here, we present evidence in support of a functional interaction of a transmembrane receptor kinase with at least one member of the plasma membrane aquaporins (PIP2F), and possibly other transporters such as the sucrose exporter SWEET11 (14). The molecular interaction of SIRK1 with aquaporins could be proven at different levels and with independent experiments: firstly, several plasma membrane intrinsic proteins were identified as interaction partners

in pull-downs of GFP-tagged SIRK1 from microsomal preparations. Secondly, a PIP2F-specific peptide served as a phosphorylation target in a kinase-substrate relationship with SIRK1. Finally, physiological analysis of water uptake properties in mutants of different expression levels of SIRK1 revealed that SIRK1 directly regulates aquaporins in a sucrose-dependent manner via phosphorylation.

SIRK1 was initially identified with rapid transient changes in protein phosphorylation in a sucrose-starvation/resupply experiment (43), and it was assumed that the early time point with maximum phosphorylation change at 3 min after sucrose resupply placed SIRK1 rather upstream in a signaling cascade. However, for protein phosphorylation and for signaling in general, 3 min is already quite long. Phosphorylation and heteromerization of receptor kinases can occur within seconds, as shown for stimulus-induced FLS2 phosphorylation and its interaction with the co-receptor BAK1 (86). Therefore, it cannot be excluded that SIRK1 activation and the response induced by SIRK1 are secondary effects of the altered osmolarity of the medium when 30 mM sucrose is resupplied to sucrose-starved seedlings.

The primary osmo-sensor in plants was identified as a histidine-receptor kinase, and connections to the MAP-kinase signaling cascade were postulated (24). Prolonged exposure of Arabidopsis plants to mild osmotic stress induced by 25 mM mannitol leads to global adjustments of protein levels also affecting mitochondrial respiration and photosynthetic proteins (27). Thus, the plant may have more than one mechanism of response to external osmotic changes, and possibly even substance-specific responses. Receptor-like protein kinases were suggested as a protein family with high potential in the context of understanding and preventing drought stress (87). Our finding that the receptor-like kinase SIRK1 is involved in the regulation of sucrose-specific osmotic responses supports this concept. Sucrose specificity of the response is suggested, as SIRK1-dependent protoplast swelling occurred after sucrose treatment, but not in *sirk1* mutant lines. No difference was observed if mannitol was used at the same osmolarity.

Proposed Model of SIRK1 Function—In general, we cannot exclude the possibility that SIRK1 functions within a larger protein complex. Particularly, the receptor kinase AT3G02880, identified as a sucrose-dependent interaction partner and phosphorylation target of SIRK1, is a candidate for the formation of a receptor complex with SIRK1. Therefore, targets identified using the *sirk1* T-DNA insertional mutant, as well as identified SIRK1 interaction partners, might in fact have to be referred to as targets and partners of a larger SIRK1 receptor complex.

In its active state, SIRK1 complex interacts with other transport proteins, particularly aquaporins (Fig. 7). Therefore, it is likely that some aquaporins are direct substrates to SIRK1, without other protein kinases being involved. There are other, recent indications for phosphorylation-dependent direct short

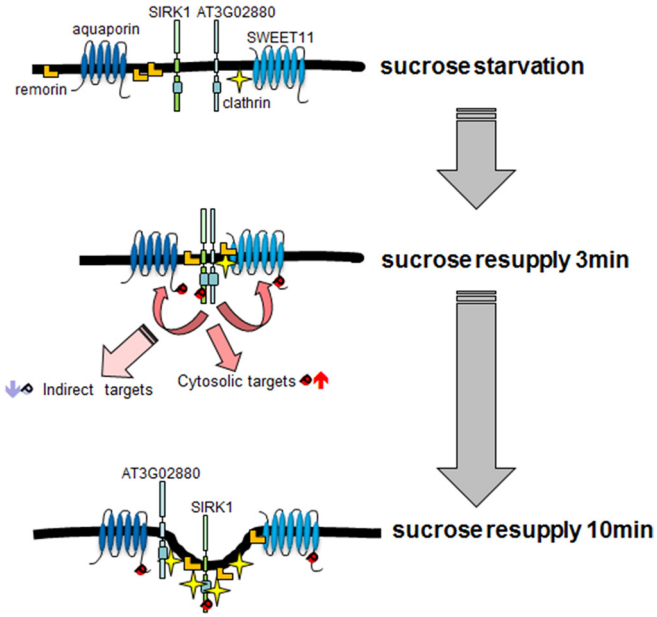

FIG. 7. **Model of SIRK1 function.** Sucrose resupply after starvation induces activation and phosphorylation of SIRK1. Active SIRK1 (independently of S744 phosphorylation) can interact with and phosphorylate aquaporin PIP2F, SWEET11, and receptor kinase AT3G02880. Further cytosolic targets and indirect targets show altered phosphorylation status. S744 phosphorylation induces favorable interaction with clathrins and promotes the internalization of SIRK1 via endocytosis.

signaling pathways at the plasma membrane involving receptor kinases (88) that mainly affected transporters—for instance, the plasma membrane H^+-ATPase. Furthermore, SIRK1 can also interact with other receptor kinases in a sucrose-dependent manner (see Table I), which suggests that SIRK1 forms heteromers under sucrose supply. The heteromerization of receptor kinases has been shown for various other plant receptor kinases (86, 89, 90). Stimulation and heteromerization can induce endocytosis, as shown for BRI1 and FLS2 (91, 92). Therefore, SIRK1 also could be targeted to endocytotic vesicles after sucrose stimulation. This hypothesis is supported by increased interaction with clathrin protein after sucrose supply and observations of increased SIRK1 endocytosis within 15 min after sucrose treatment (see Table I and Fig. 6).

An interesting finding in this study was the interaction of SIRK1 with remorin proteins and indications that remorins also are phosphorylation targets of SIRK1. Remorins are considered as marker proteins for sterol-rich membrane microdomains (69, 70), also known as ordered lipid phases within the membrane. Stimulus-dependent phosphorylation of remorins was also found upon elicitor treatment of plant cell cultures (37), as well as in other phosphoproteomic studies (41, 93). A possible function of the interaction of SIRK1 with remorins could be in the recruitment of SIRK1 and its target proteins to the same ordered lipid phase, or the formation of a functional SIRK1 protein complex. Such rearrangements of signaling

proteins, particularly of receptor kinases, between the lipid-ordered phase and the disordered phase (94) were demonstrated in mammalian systems for the EGF receptor, which is recruited to the membrane-ordered phase before inactivation and endocytosis (95). Also, the phosphorylation-dependent phase transition and subsequent assembly of signaling complexes in the Nck-signaling pathway (96) suggests that such stimulus-dependent recruitment of proteins to particular lipid and protein environments might represent a general regulatory principle in all organisms. In plants, phosphorylation-dependent recruitment of protein–protein interaction partners specifically to sterol-rich membrane microdomains has recently been demonstrated for the anion channel SLAH3 and its phosphorylating kinase CPK21 (97). We propose similar mechanisms for SIRK1 and its associated proteins in interactions with clathrins for internalization.

Besides transport proteins and other receptor-like kinases, the candidate targets to SIRK1 included a number of soluble proteins, and even proteins of internal membranes, such as the Golgi or tonoplast. The identification of SnRK2.5 suggests a link to further cytosolic signaling cascades. Members of the SnRK family were previously associated with signaling in relation to metabolic stresses (98, 99), and in particular the SnRK2 kinases were suggested to function in intracellular osmotic responses (26). There are indications that phosphorylation is required for the activation of SnRK2.5, but the precise sites of activation are not yet identified (25). Two members of the soluble BSK kinase family were identified as interaction partners to SIRK1 but did not show up as differentially phosphorylated. BSK1 and BSK2 were initially characterized as members of the brassinosteroid signaling pathway induced by receptor kinase BRI1 (68). BSKs are activated by phosphorylation by the receptor kinase BRI1 (90), but other receptor kinases, such as SIRK1, also might activate BSK signaling.

The identification of several ribosomal proteins as candidate targets for SIRK1 suggests a direct link to adjustments of protein synthesis rates under altered sucrose environments. In other studies, it was found that ribosomal proteins are recruited to polysomes at the onset of the light period in a diurnal cycle (100). Polysome levels correlated with sucrose concentration in the leaf (101). Furthermore, diurnal changes in ribosomal protein phosphorylation have been described (102). This suggests that sucrose indeed might play an important role in inducing alterations in the translational machinery, either via the recruitment of ribosomes to polysomes or through alterations in ribosomal complex composition (18). However, ribosomal proteins are frequently co-purified with membrane proteins and constitute typical background proteins in pull-downs. Therefore, results regarding direct connections of SIRK1 to protein synthesis require further verification.

It is likely that among the soluble proteins and proteins localized to internal membranes, there are several indirect targets of the SIRK1 complex. In particular, proteins in tonoplast membrane (*e.g.* ERD6) are likely to be phosphorylated by another kinase, and not by SIRK1 directly. Also, the identification of several proteins from central carbohydrate metabolism with increased phosphorylation levels in the *sirk1* mutant indicates that the removal of SIRK1 has indirect effects beyond direct interactions of SIRK1 within the membrane context. It is interesting, however, that also among the indirect targets there is a strong link to the sucrose stimulus used in this experiment. Thus, positive (activating) as well as negative (inhibition) regulatory interactions are involved in sucrose-induced responses mediated by SIRK1 and its complex.

Role of SIRK1 Phosphorylation Site S744—The phosphorylation of SIRK1 at S744 does not directly affect target protein phosphorylation efficiency, but it is suggested to create a suitable environment for the SIRK1 kinase itself, for example, through recruitment to different lipid environments of the plasma membrane (96) or as interaction sites for activating partner proteins (Fig. 6). Based on the observation that $SIRK^{S744D}$ mutants show sucrose-independent SIRK1 endocytotic activity, we propose a role of S744 phosphorylation in SIRK1 internalization. A significant degree of S744 phosphorylation must be present for efficient internalization of SIRK1. It remains unclear whether SIRK1 internalization will include the complete functional complex or whether specifically only SIRK1 is removed from the membrane. Detailed roles of the phosphorylation-specific interaction partners will have to be determined using other methods, such as peptide specific interaction screens (103) and cell biological studies of membrane microdomain locations of SIRK1 and its interactors. The functional model of SIRK1 (Fig. 7) implies that sucrose resupply after starvation induces activation and phosphorylation of SIRK1. Active SIRK1, independently of S744 phosphorylation, can interact with and phosphorylate aquaporin PIP2F and SWEET11, as well as receptor kinase AT3G02880. Further cytosolic targets and indirect targets show altered phosphorylation status in a SIRK1-dependent manner. S744 phosphorylation increases favorable interaction with clathrins and promotes the internalization of SIRK1 via endocytosis. It cannot be ruled out that the activation of SIRK1 depends either on other, not identified phosphorylation sites or sucrose-induced interaction partners. Notably, interacting RLK AT3G02880 also shows sucrose-induced phosphorylation changes (43), and for both proteins (SIRK1 as well as AT3G02880), these phosphorylation sites lie within a phosphorylation hotspot (104).

The transient nature of observed sucrose-induced phosphorylation (43) creates a challenge in experimentally unraveling SIRK1 activation, functional SIRK1 complex formation, and subsequent SIRK1 internalization. These processes most likely occur at different time scales that might not have been adequately captured in all cases by studying the 3-min stimulation time point of maximum sucrose-induced SIRK1 phosphorylation.

CONCLUSIONS

Results from this work provide an example for the existence of membrane-located signaling interactions consisting of a receptor kinase and a transmembrane transporter as substrate. Possibly, SIRK1 has a dual role in the direct regulation of plasma membrane proteins, as well as in interactions with intracellular signaling pathways. In addition, we present a functional context of a yet uncharacterized transmembrane receptor kinase with respect to sucrose-dependent responses. These findings are based on comparative quantitative protein phosphorylation profiling of kinase knock-out mutants as the discovery phase in combination with a conditional analysis of protein–protein interactions of tagged kinase protein overexpressed in the mutant background. Finally, high-level suitable physiological and cell biological experiments were applied in order to pinpoint the functional and mechanistic context of SIRK1 receptor kinase function. With the combination of these methods, new insights into the function of other as yet uncharacterized protein kinases are feasible in the future.

Acknowledgments—We thank Staffan Persson for fruitful discussions throughout the progress of this work. The technicians Kerstin Zander and Margitta Schümann are acknowledged for their valuable assistance with large-scale seedling liquid culture experiments. Guangyou Duan helped with statistical analyses of phosphorylation patterns, and Dandan Lu assisted during large numbers of sample preparations.

* This project was financed through a DFG Emmy-Noether Fellowship awarded to W.X.S.

S This article contains supplemental material.

Author contributions: X.N.W. carried out the main wet lab work (cloning of constructs, seedling liquid cultures, proteomics experiments, LC-MS/MS analysis) and performed proteomic data analysis. C.S.R. performed the confocal microscopy contributing to Figs. 1*D* and 6. H.P.O. designed the peptides for *in vitro* kinase assays and contributed to kinase activity assay measurements and plasma membrane preparations. G.O. contributed to protoplast swelling assays and the image analysis of protoplasts. W.X.S. provided strategic supervision of the project, helped with mass spectrometric analysis of samples, and mainly wrote the manuscript.

REFERENCES

1. Chapin, F. S., Schulze, E. D., and Mooney, H. A. (1990) The ecology and economics of storage in plants. *Annu. Rev. Ecol. Syst.* **21,** 423–447
2. Cheng, C.-L., Acedo, G. N., Christinsin, M., and Conkling, M. A. (1992) Sucrose mimics the light induction of *Arabidopsis* nitrate reductase gene transcription. *Proc. Natl. Acad. Sci. U.S.A.* **89,** 1861–1864
3. Dijkwel, P. P., Huijser, C., Weisbeek, P. J., Chua, N. H., and Smeekens, S. C. M. (1997) Sucrose control of phytochrome A signaling in *Arabidopsis. Plant Cell* **9,** 583–595
4. Chiou, T. J., and Bush, D. R. (1998) Sucrose is a signal molecule in assimilate partitioning. *Proc. Natl. Acad. Sci. U.S.A.* **95,** 4784–4788
5. Rook, F., Gerrits, N., Kortsett, A., van Kampe, M., and Borrias, M. (1998) Sucrose specific signalling represses translation of the Arabidopsis *ATB2* bZIP transcription factor gene. *Plant J.* **15,** 256–263
6. Huber, S. C., and Huber, J. L. (1996) Role and regulation of sucrose-phosphate-synthase in higher plants. *Annu. Rev. Plant Physiol. Plant Mol. Biol.* **47,** 431–444
7. Loewe, A., Einig, W., and Hampp, R. (1996) Coarse and fine control and annual changes of sucrose-phosphate synthase in Norway spruce needles. *Plant Physiol.* **112,** 641–649
8. Winter, H., and Huber, S. C. (2000) Regulation of sucrose metabolism in higher plants: localization and regulation of activity of key enzymes. *Crit. Rev. Biochem. Mol. Biol.* **35,** 253–289
9. Kühn, C., Quick, W. P., Schulz, A., Riesmeier, J. W., Sonnewald, U., and Frommer, W. B. (1996) Companion cell-specific inhibition of the potato sucrose transporter SUT1. *Plant Cell Environ.* **19,** 1115–1123
10. Stadler, R., Truernit, E., Gahrtz, M., and Sauer, N. (1999) The AtSUC1 sucrose carrier may represent the osmotic driving force for anther dehiscence and pollen tube growth in *Arabidopsis. Plant J.* **19,** 269–278
11. Lemoine, R. (2000) Sucrose transporters in plants: update on function and structure. *Biochim. Biophys. Acta* **1465,** 246–262
12. Schulze, W., Weise, A., Frommer, W. B., and Ward, J. M. (2000) Function of the cytosolic N-terminus of sucrose transporter AtSUT2 in substrate affinity. *FEBS Lett.* **485,** 189–194
13. Eckardt, N. A. (2003) The function of SUT2/SUC3 sucrose transporters: the debate continues. *Plant Cell* **14,** 1259–1262
14. Chen, L. Q., Qu, X. Q., Hou, B. H., Sosso, D., Osorio, S., Fernie, A. R., and Frommer, W. B. (2011) Sucrose efflux mediated by SWEET proteins as a key step for phloem transport. *Science* **35,** 207–211
15. Wind, J., Smeekens, S., and Hanson, J. (2010) Sucrose: metabolite and signaling molecule. *Phytochem.* **71,** 1510–1614
16. Osuna, D., Usadel, B., Morcuende, R., Gibon, Y., Bläsing, O. E., Höhne, M., Günter, M., Kamlage, B., Trethewey, R., Scheible, W. R., and Stitt, M. (2007) Temporal responses of transcripts, enzyme activities and metabolites after adding sucrose to carbon-deprived Arabidopsis seedlings. *Plant J.* **49,** 463–491
17. Nicolai, M., Roncato, M. A., Canoy, A. S., Roquie, D., Sarda, X., Freyssinet, G., and Robaglia, C. (2006) Large-scale analysis of mRNA translation states during sucrose starvation in Arabidopsis cells identifies cell proliferation and chromatin structure as targets of translational control. *Plant Physiol.* **141,** 663–673
18. Hummel, M., Cordewener, J. H., de Groot, J. C., Smeekens, S., America, A. H., and Hanson, J. (2012) Dynamic protein composition of Arabidopsis thaliana cytosolic ribosomes in response to sucrose feeding as revealed by label free MSE proteomics. *Proteomics* **12,** 1024–1038
19. Smeekens, S. C. M. (2000) Sugar-induced signal transduction in plants. *Annu. Rev. Plant Physiol. Plant Mol. Biol.* **51,** 49–81
20. Ma, J., Hanssen, M., Lundgren, K., Hernández, L., Delatte, T., Ehlert, A., Liu, C. M., Schluepmann, H., Dröge-Laser, W., Moritz, T., Smeekens, S., and Hanson, J. (2011) The sucrose-regulated Arabidopsis transcription factor bZIP11 reprograms metabolism and regulates trehalose metabolism. *New Phytol.* **191,** 733–745
21. Barker, L., Kühn, C., Weise, A., Schulz, A., Gebhardt, C., Hirner, B., Hellmann, H., Schulze, W., Ward, J. M., and Frommer, W. B. (2000) SUT2, a putative sucrose sensor in sieve elements. *Plant Cell* **12,** 1153–1164
22. Reinders, A., Schulze, W., Thaminy, S., Stagljar, I., Frommer, W. B., and Ward, J. M. (2002) Intra- and intermolecular interactions in sucrose transporters at the plasma membrane detected by the split-ubiquitin system and functional assays. *Structure* **10,** 763–772
23. Jang, J. C., León, P., Zhou, L., and Sheen, J. (1997) Hexokinase as a sugar sensor in higher plants. *Plant Cell* **9,** 5–19
24. Urao, T., Yakubov, B., Satoh, R., Yamaguchi-Shinozaki, K., Seki, M., Hirayama, T., and Shinozaki, K. (1999) A transmembrane hybrid-type histidine kinase in *Arabidopsis* functions as an osmosensor. *Plant Cell* **11,** 1743–1754
25. Boudsocq, M., Droillard, M. J., Barbier-Brygoo, H., and Laurière, C. (2007) Different phosphorylation mechanisms are involved in the activation of sucrose non-fermenting 1 related protein kinases 2 by osmotic stresses and abscisic acid. *Plant Mol. Biol.* **63,** 491–503
26. Fujii, H., Verslues, P. E., and Zhu, J. K. (2011) Arabidopsis decuple mutant reveals the importance of SnRK2 kinases in osmotic stress responses in vivo. *Proc. Natl. Acad. Sci. U.S.A.* **108,** 1717–1722
27. Skirycz, A., Memmi, S., De Bodt, S., Maleux, K., Obata, T., Fernie, A. R., Devreese, B., and Inzé, D. (2011) A reciprocal 15N-labeling proteomic analysis of expanding Arabidopsis leaves subjected to osmotic stress indicates importance of mitochondria in preserving plastid functions. *J. Proteome Res.* **10,** 1018–1029
28. Prak, S., Hem, S., Boudet, J., Viennois, G., Sommerer, N., Rossignol, M., Maurel, C., and Santoni, V. (2008) Multiple phosphorylations in the

C-terminal tail of plant plasma membrane aquaporins: role in subcellular trafficking of AtPIP2;1 in response to salt stress. *Mol. Cell. Proteomics* **7,** 1019–1030
29. Shapiguzov, A., Lyukevich, A. A., Allakhverdiev, S. I., Sergeyenko, T. V., Suzuki, I., Murata, N., and Los, D. A. (2005) Osmotic shrinkage of cells of Synechocystis sp. PCC 6803 by water efflux via aquaporins regulates osmostress-inducible gene expression. *Microbiology* **151,** 447–455
30. Sommer, A., Geist, B., Da Ines, O., Gehwolf, R., Schäffner, A. R., and Obermeyer, G. (2008) Ectopic expression of Arabidopsis thaliana plasma membrane intrinsic protein 2 aquaporins in lily pollen increases the plasma membrane water permeability of grain but not of tube protoplasts. *New Phytol.* **180,** 787–797
31. Tornroth-Horsefield, S., Wang, Y., Hedfalk, K., Johanson, U., Karlsson, M., Tajkhorshid, E., Neutze, R., and Kjellbom, P. (2006) Structural mechanism of plant aquaporin gating. *Nature* **439,** 688–694
32. Kline-Jonakin, K. G., Barrett-Wilt, G. A., and Sussman, M. R. (2011) Quantitative plant phosphoproteomics. *Curr. Opin. Plant Biol.* **14,** 507–511
33. Schulze, W. (2010) Proteomics approaches to understand protein phosphorylation in pathway modulation. *Curr. Opin. Plant Biol.* **13,** 1–8
34. Toroser, D., Athwal, G. S., and Huber, S. C. (1998) Site-specific regulatory interaction between spinach leaf sucrose-phosphate synthase and 14–3-3 proteins. *FEBS Lett.* **435,** 110–114
35. Roblin, G., Sakr, S., Bonmort, J., and Delrot, S. (1998) Regulation of a plant plasma membrane sucrose transporter by phosphorylation. *FEBS Lett.* **424,** 165–168
36. Ransom-Hodgkins, W. D., Vaughn, M. W., and Bush, D. R. (2003) Protein phosphorylation plays a key role in sucrose-mediated transcriptional regulation of a phloem-specific proton-sucrose symporter. *Planta* **217,** 483–489
37. Benschop, J. J., Mohammed, S., O'Flaherty, M., Heck, A. J., Slijper, M., and Menke, F. L. (2007) Quantitative phospho-proteomics of early elicitor signalling in Arabidopsis. *Mol. Cell. Proteomics* **6,** 1705–1713
38. Chen, E. I., Hewel, J., Felding-Habermann, B., and Yates, J. R. I. (2006) Large scale protein profiling by combination of protein fractionation and multidimensional protein identification technology (MudPIT). *Mol. Cell. Proteomics* **5,** 53–56
39. Engelsberger, W. R., and Schulze, W. X. (2012) Nitrate and ammonium lead to distinct global dynamic phosphorylation patterns when resupplied to nitrogen starved Arabidopsis seedlings. *Plant J.* **69,** 978–995
40. Kline, K. G., Barrett-Wilt, G. A., and Sussman, M. R. (2010) In planta changes in protein phosphorylation induced by the plant hormone abscisic acid. *Proc. Natl. Acad. Sci. U.S.A.* **107,** 15986–15991
41. Reiland, S., Messerli, G., Baerenfäller, K., Gerrits, B., Endler, A., Grossmann, J., Gruissem, W., and Baginsky, S. (2009) Large-scale Arabidopsis phosphoproteome profiling reveals novel chloroplast kinase substrates and phosphorylation networks. *Plant Physiol.* **150,** 889–903
42. Nühse, T. S., Bottrill, A. R., Jones, A. M., and Peck, S. C. (2007) Quantitative phosphoproteomic analysis of plasma membrane proteins reveals regulatory mechanisms of plant innate immune responses. *Plant J.* **51,** 931–940
43. Niittylä, T., Fuglsang, A. T., Palmgren, M. G., Frommer, W. B., and Schulze, W. X. (2007) Temporal analysis of sucrose-induced phosphorylation changes in plasma membrane proteins of Arabidopsis. *Mol. Cell. Proteomics* **6,** 1711–1726
44. Durek, P., Schmidt, R., Heazlewood, J. L., Jones, A., MacLean, D., Nagel, A., Kersten, B., and Schulze, W. X. (2010) PhosPhAt: the Arabidopsis thaliana phosphorylation site database. An update. *Nucleic Acids Res.* **38,** D828–D834
45. Heazlewood, J. L., Durek, P., Hummel, J., Selbig, J., Weckwerth, W., Walther, D., and Schulze, W. X. (2008) PhosPhAt: a database of phosphorylation sites in Arabidopsis thaliana and a plant-specific phosphorylation site predictor. *Nucleic Acids Res.* **36,** D1015-D1021
46. Huang, Y., Houston, N. L., Tovar-Mendez, A., Stevenson, S. E., Miernyk, J. A., Randall, D. D., and Thelen, J. J. (2010) A quantitative mass spectrometry-based approach for identifying protein kinase-clients and quantifying kinase activity. *Anal. Biochem.* **402,** 69–76
47. Feilner, T., Hultschig, C., Lee, J. M., Meyer, S., Immink, R. G. H., Koenig, A., Possling, A., Seitz, H., Beveridge, A., Scheel, D., Cahill, d. J., Lehrach, H., Kreutzberger, J., and Kersten, B. (2005) High throughput identification of potential Arabidopsis mitogen-activated protein kinases substrates. *Mol. Cell. Proteomics* **4,** 1558–1568
48. Vlad, F., Turk, B. E., Peynot, P., Leung, J., and Merlot, S. (2008) A versatile strategy to define the phosphorylation preferences of plant protein kinases and screen for putative substrates. *Plant J.* **55,** 104–117
49. Zulawski, M., Braginets, R., and Schulze, W. X. (2013) PhosPhAt goes kinases—searchable protein kinase target information in the plant phosphorylation site database PhosPhAt. *Nucleic Acids Res.* **41,** D1176–D1184
50. Alonso, J. M., Stepanova, A. N., Leisse, T. J., Kim, C. J., Chen, H., Shinn, P., Stevenson, D. K., Zimmerman, J., Barajas, P., Cheuk, R., Gadrinab, C., Heller, C., Jeske, A., Koesema, E., Meyers, C. C., Parker, H., Prednis, L., Ansari, Y., Choy, N., Deen, H., Geralt, M., Hazari, N., Hom, E., Karnes, M., Mulholland, C., Ndubaku, R., Schmidt, I., Guzman, P., Aguilar-Henonin, L., Schmid, M., Weigel, D., Carter, D. E., Marchand, T., Risseeuw, E., Brogden, D., Zeko, A., Crosby, W. L., Berry, C. C., and Ecker, J. R. (2003) Genome-wide insertional mutagenesis of Arabidopsis thaliana. *Science* **301,** 653–657
51. Schmittgen, T. D., and Livak, K. J. (2008) Analyzing real-time PCR data by the comparative C(T) method. *Nat. Protoc.* **3,** 1101–1108
52. Clough, S. J., and Bent, A. F. (1998) Floral dip: a simplified method for *Agrobacterium*-mediated transformation of *Arabidopsis thaliana. Plant J.* **16,** 735–743
53. Jouanneau, J. P., and Peaud-Lenoel, C. (1967) Growth and synthesis of proteins in cell suspensions of a kinetin dependent tobacco. *Physiol. Plant* **20,** 834–850
54. Sommer, A., Mahlknecht, G., and Obermeyer, G. (2007) Measuring the osmotic water permeability of the plant protoplast plasma membrane: implication of the nonosmotic volume. *J. Membr. Biol.* **215,** 111–123
55. Robert, S., Kleine-Vehn, J., Barbez, E., Sauer, M., Paciorek, T., Baster, P., Vanneste, S., Zhang, J., Simon, S., Čovanová, M., Hayashi, K., Dhonukshe, P., Yang, Z., Bednarek, S. Y., Jones, A. M., Luschnig, C., Aniento, F., Zažímalová, E., and Friml, J. (2010) ABP1 mediates auxin inhibition of clathrin-dependent endocytosis in Arabidopsis. *Cell* **143,** 111–121
56. Rappsilber, J., Ishihama, Y., and Mann, M. (2003) Stop and go extraction tips for matrix-assisted laser desorption/ionization, nanoelectrospray, and LC/MS sample pretreatment in proteomics. *Anal. Chem.* **75,** 663–670
57. Larsen, M. R., Thingholm, T. E., Jensen, O. N., Roepstorff, P., and Jorgensen, T. J. D. (2005) Highly selective enrichment of phosphorylated peptides from peptide mixtures using titanium dioxide microcolumns. *Mol. Cell. Proteomics* **4,** 873–886
58. Nakagami, H., Sugiyama, N., Mochida, K., Daudi, A., Yoshida, Y., Toyoda, T., Tomita, M., Ishihama, Y., and Shirasu, K. (2010) Large-scale comparative phosphoproteomics identifies conserved phosphorylation sites in plants. *Plant Physiol.* **153,** 1161–1174
59. Schroeder, M. J., Shabanowitz, J., Schwartz, J. C., Hunt, D. F., and Coon, J. J. (2004) A neutral loss activation method for improved phosphopeptide sequence analysis by quadrupole ion trap mass spectrometry. *Anal. Chem.* **76,** 3590–3598
60. Cox, J., and Mann, M. (2008) MaxQuant enables high peptide identification rates, individualized p.p.b.-range mass accuracies and proteome-wide protein quantification. *Nat. Biotechnol.* **26,** 1367–1372
61. Cox, J., Neuhauser, N., Michalski, A., Scheltema, R. A., Olsen, J. V., and Mann, M. (2011) Andromeda: a peptide search engine integrated into the MaxQuant environment. *J. Proteome Res.* **10,** 1794–1805
62. Zauber, H., and Schulze, W. X. (2012) Proteomics wants cRacker: automated standardized data analysis of LC/MS derived proteomic data. *J. Proteome Res.* **11,** 5548–5555
63. Schulze, W. X., Schneider, T., Starck, S., Martinoia, E., and Trentmann, O. (2012) Cold acclimation induces changes in Arabidopsis tonoplast protein abundance and activity and alters phosphorylation of tonoplast monosaccharide transporters. *Plant J.* **69,** 529–541
64. Benjamini, Y., and Hochberg, Y. (1995) Controlling the false discovery rate: a practical and powerful approach to multiple testing. *J. R. Stat. Soc.* **57,** 289–300
65. Thimm, O., Bläsing, O., Gibon, Y., Nagel, A., Meyer, S., Kruger, P., Selbig, J., Muller, L. A., Rhee, S. Y., and Stitt, M. (2004) MAPMAN: a user-driven tool to display genomics data sets onto diagrams of metabolic pathways and other biological processes. *Plant J.* **37,** 914–939
66. Tanz, S. K., Castleden, I., Hooper, C. M., Vacher, M., Small, I., and Millar,

H. A. (2013) SUBA3: a database for integrating experimentation and prediction to define the SUBcellular location of proteins in Arabidopsis. *Nucleic Acids Res.* **41,** D1185–D1191
67. Schwartz, D., and Gygi, S. P. (2005) An iterative statistical approach to the identification of protein phosphorylation motifs from large-scale data sets. *Nat. Biotechnol.* **23,** 1391–1398
68. Tang, W., Kim, T.-W., Oses-Prieto, J. A., Sun, Y., Deng, Z., Zhu, S., Wang, R., Burlingam, A., and Wang, Z.-Y. (2008) BSKs mediate signal transduction from the receptor kinase BRI1 in Arabidopsis. *Science* **321,** 557–560
69. Kierszniowska, S., Seiwert, B., and Schulze, W. X. (2009) Definition of Arabidopsis sterol-rich membrane microdomains by differential treatment with methyl-β-cyclodextrin and quantitative proteomics. *Mol. Cell. Proteomics* **8,** 612–623
70. Raffaele, S., Bayer, E., Lafarge, D., Cluzet, S., German Retana, S., Boubekeur, T., Leborgne-Castel, N., Carde, J. P., Lherminier, J., Noirot, E., Satiat-Jeunemaitre, B., Laroche-Traineau, J., Moreau, P., Ott, T., Maule, A. J., Reymond, P., Simon-Plas, F., Farmer, E. E., Bessoule, J. J., and Mongrad, S. (2009) Remorin, a Solanaceae protein resident in membrane rafts and plasmodesmata, impairs potato virus X movement. *Plant Cell* **21,** 1541–1555
71. Shiu, S.-H., and Bleecker, A. B. (2001) Receptor-like kinases form *Arabidopsis* form a monophyletic gene family related to animal receptor kinases. *Proc. Natl. Acad. Sci. U.S.A.* **98,** 10763–10768
72. Wang, Z.-Y., Seto, H., Fijioka, S., Yoshida, S., and Chory, J. (2001) BRI1 is a critical component of a plasma-membrane receptor for plant steroids. *Nature* **410,** 380–383
73. Gomez-Gomez, L., Felix, G., and Boller, T. (2000) FLS2: an LRR receptor-like kinase involved in the perception of the bacterial elicitor flagellin in Arabidopsis. *Mol. Cell* **5,** 1003–1011
74. Trotochaud, A. E., Hao, T., Wu, G., Yang, Z., and Clark, S. E. (1999) The CLAVATA1 receptor-like kinase requires CLAVATA3 for this assembly into a signaling complex that includes KAPP and Rho-related protein. *Plant Cell* **11,** 299–301
75. Scheer, J. M., and Ryan, C. A. (2002) The systemin receptor SR160 from *Lycopersicon peruvianum* is a member of the LRR receptor kinase family. *Proc. Natl. Acad. Sci. U.S.A.* **99,** 9585–9590
76. Stührwohldt, N., Dahlke, R. I., Steffens, B., Johnson, A., and Sauter, M. (2011) Phytosulfokine-α controls hypocotyl length and cell expansion in Arabidopsis thaliana through Phytosulfokine receptor 1. *PLoS One* **6,** e21054
77. Oh, M. H., Wang, X., Kota, U., Goshe, M. B., Clouse, S. D., and Huber, S. C. (2010) Tyrosine phosphorylation of the BRI1 receptor kinase emerges as a component of brassinosteroid signaling in Arabidopsis. *Proc. Natl. Acad. Sci. U.S.A.* **106,** 658–663
78. Wang, X., Goshe, M. B., Sonderblom, E. J., Phinney, B. S., Kuchar, J. A., Li, J., Asami, T., Yoshida, S., Huber, S. C., and Clouse, S. D. (2005) Identification and functional analysis of in vivo phosphorylation sites of the Arabidopsis Brassinosteroid-insensitive 1 receptor kinase. *Plant Cell* **17,** 1685–1703
79. Dephoure, N., Howson, R. W., Blethrow, J. D., Shokat, K. M., and O'Shea, E. K. (2005) Combining chemical genetics and proteomics to identify protein kinase substrates. *Proc. Natl. Acad. Sci. U.S.A.* **102,** 17940–17945
80. Shah, K., Liu, Y., Deirmengian, C., and Shokat, K. M. (1997) Engineering unnatural nucleotide specificity for Rous sarcoma virus tyrosine kinase to uniquely label its direct substrates. *Proc. Natl. Acad. Sci. U.S.A.* **94,** 3565–3570
81. Morandell, S., Grosstessner-Hain, K., Roitinger, E., Hudecz, O., Lindhorst, T., Teis, D., Wrulich, O. A., Mazanek, M., Taus, T., Ueberall, F., Mechtler, K., and Huber, L. A. (2010) QIKS—quantitative identification of kinase substrates. *Proteomics* **10,** 2015–2025
82. Pan, C., Gnad, F., Olsen, J. V., and Mann, M. (2008) Quantitative phosphoproteome analysis of a mouse liver cell line reveals specificity of phosphatase inhibitors. *Proteomics* **8,** 4534–4546
83. Daub, H., Olsen, J. V., Bairlein, M., Gnad, F., Oppermann, F. S., Körner, R., Greff, Z., Kéri, G., Stemmann, O., and Mann, M. (2008) Kinase-selective enrichment enables quantitative phosphoproteomics of the kinome across the cell cycle. *Mol. Cell* **31,** 438–448
84. Gordus, A., Krall, J. A., Beyer, E. M., Kaushansky, A., Wolf-Yadlin, A., Sevecka, M., Chang, B. H., Rush, J., and MacBeath, G. (2008) Linear combinations of docking affinities explain quantitative differences in RTK signaling. *Mol. Syst. Biol.* **5,** 1–10
85. Bodenmiller, B., Wanka, S., Kraft, C., Urban, J., Campbell, D., Pedrioli, P. G., Gerrits, B., Picotti, P., Lam, H., Vitek, O., Brusniak, M. Y., Roschitzki, B., Zhang, C., Shokat, K. M., Schlapbach, R., Colman-Lerner, A., Nolan, G. P., Nesvizhskii, A. I., Peter, M., Loewith, R., von Mering, C., and Aebersold, R. (2010) Phosphoproteomic analysis reveals interconnected system-wide responses to perturbations of kinases and phosphatases in yeast. *Sci. Signal.* **3,** rs4
86. Schulze, B., Mentzel, T., Jehle, A. K., Müller, K., Beeler, S., Boller, T., Felix, G., and Chinchilla, D. (2010) Rapid heteromerization and phosphorylation of ligand-activated plant transmembrane receptors and their associated kinase BAK1. *J. Biol. Chem.* **285,** 9444–9451
87. Marshall, A., Aalen, R. B., Audenaert, D., Beeckman, T., Broadley, M. R., Butenko, M. A., Caño-Delgado, A. I., de Vries, S., Dresselhaus, T., Felix, G., Graham, N. S., Foulkes, J., Granier, C., Greb, T., Grossniklaus, U., Hammond, J. P., Heidstra, R., Hodgman, C., Hothorn, M., Inzé, D., Ostergaard, L., Russinova, E., Simon, R., Skirycz, A., Stahl, Y., Zipfel, C., and De Smet, I. (2012) Tackling drought stress: receptor-like kinases present new approaches. *Plant Cell* **24,** 2262–2278
88. Caesar, K., Elgass, K., Chen, Z., Huppenberger, P., Witthöft, J., Schleifenbaum, F., Blatt, M. R., Oecking, C., and Harter, K. (2011) A fast brassinolide-regulated response pathway in the plasma membrane of Arabidopsis thaliana. *Plant J.* **66,** 528–540
89. Bleckmann, A., Weidtkamp-Peters, S., Seidel, C. A., and Simon, R. (2010) Stem cell signaling in Arabidopsis requires CRN to localize CLV2 to the plasma membrane. *Plant Physiol.* **152,** 166–176
90. Kim, T. W., Guan, S., Sun, Y., Deng, Z., Tang, W., Shang, J. X., Sun, Y., Burlingam, A., and Wang, Z. Y. (2009) Brassinosteroid signal transduction from cell-surface receptor kinases to nuclear transcription factors. *Nat. Cell Biol.* **11,** 1254–1260
91. Russinova, E., Borst, J. W., Kwaaitaal, M., Cano-Delgado, A., Yin, Y., Chory, J., and De Vries, S. C. (2004) Heterodimerization and endocytosis of Arabidopsis brassinosteroid receptors BRI1 and AtSERK3 (BAK1). *Plant Cell* **16,** 3216–3229
92. Beck, M., Zhou, J., Faulkner, C., Maclean, D., and Robatzek, S. (2012) Spatio-temporal cellular dynamics of the Arabidopsis flagellin receptor reveal activation status-dependent endosomal sorting. *Plant Cell* **24,** 4205–4219
93. Sugiyama, N., Nakagami, H., Mochida, K., Daudi, A., Tomita, M., Shirasu, K., and Ishihama, Y. (2008) Large-scale phosphorylation mapping reveals the extent of tyrosine phosphorylation in *Arabidopsis. Mol. Syst. Biol.* **4,** e1–e7
94. Lingwood, D., and Simons, K. (2010) Lipid rafts as a membrane-organizing principle. *Science* **327,** 46–50
95. Coskun, Ü., Grzybek, M., Drechsel, D., and Simons, K. (2011) Regulation of human EGF receptor by lipids. *Proc. Natl. Acad. Sci. U.S.A.* **108,** 9044–9048
96. Li, P., Banjade, S., Cheng, H. C., Kim, S., Chen, B., Guo, L., Llaguno, M., Hollingsworth, J. V., King, D. S., Banani, S. F., Russo, P. S., Jiang, Q. X., Nixon, B. T., and Rosen, M. K. (2012) Phase transitions in the assembly of multivalent signalling proteins. *Nature* **483,** 336–340
97. Demir, F., Hontrich, C., Blachutzik, J. O., Scherzer, S., Reinders, Y., Kierszniowska, S., Schulze, W. X., Harms, G. S., Hedrich, R., Geiger, D., and Kreuzer, I. (2013) Arabidopsis nanodomain-delimited ABA signaling pathway regulates the anion channel SLAH3. *Proc. Natl. Acad. Sci. U.S.A.* **110,** 8296–8301
98. Halford, N. G., and Hey, S. J. (2009) Snf1-related protein kinases (SnRKs) act within an intricate network that links metabolic and stress signalling in plants. *Biochem. J.* **419,** 247–259
99. Shin, R., Alvarez, S., Burch, A. Y., Jez, J. M., and Schachtman, D. P. (2007) Phosphoproteomic identification of targets of the Arabidopsis sucrose nonfermenting-like kinase SnRK2.8 reveals a connection to metabolic processes. *Proc. Natl. Acad. Sci. U.S.A.* **104,** 6460–6465
100. Piques, M. C., Schulze, W. X., Höhne, M., Usadel, B., Gibon, Y., Rohwer, J., and Stitt, M. (2009) Ribosome and transcript copy numbers, polysome occupancy and enzyme dynamics in Arabidopsis. *Mol. Syst. Biol.* **5,** E1–E17
101. Pal, S. K., Liput, M., Piques, M., Ishihara, H., Obata, T., Martins, M. C.,

Sulpice, R., van Dongen, J. T., Fernie, A. R., Yadav, U. P., Lunn, J. E., Usadel, B., and Stitt, M. (2013) Diurnal changes of polysome loading track sucrose content in the rosette of wildtype Arabidopsis and the starchless pgm mutant. *Plant Physiol.* **162,** 1246–1265

102. Turkina, M. V., Klang Årstrand, H., and Vener, A. V. (2011) Differential phosphorylation of ribosomal proteins in Arabidopsis thaliana plants during day and night. *PLoS One* **6,** e29307
103. Schulze, W. X., and Mann, M. (2004) A novel proteomic screen for peptide-protein interactions. *J. Biol. Chem.* **279,** 10756–10764
104. Christian, J. O., Braginets, R., Schulze, W. X., and Walther, D. (2012) Characterization and prediction of protein phosphorylation hotspots in Arabidopsis thaliana. *Front. Plant Sci.* **3,** 207